Heterogeneity of Ca^{2+} Gating of Skeletal Muscle and Cardiac Ryanodine Receptors

Julio A. Copello, Sebastian Barg, Hitoshi Onoue, and Sidney Fleischer
Department of Molecular Biology, Vanderbilt University, Nashville, Tennessee 37235 USA

ABSTRACT The single-channel activity of rabbit skeletal muscle ryanodine receptor (skeletal RyR) and dog cardiac RyR was studied as a function of cytosolic [Ca^{2+}]. The studies reveal that for both skeletal and cardiac RyRs, heterogeneous populations of channels exist, rather than a uniform behavior. Skeletal muscle RyRs displayed two extremes of behavior: 1) low-activity RyRs (LA skeletal RyRs, ~35% of the channels) had very low open probability ($P_o < 0.1$) at all [Ca^{2+}] and remained closed in the presence of Mg^{2+} (2 mM) and ATP (1 mM); 2) high-activity RyRs (HA skeletal RyRs) had much higher activity and displayed further heterogeneity in their P_o values at low [Ca^{2+}] (<50 nM), and in their patterns of activation by [Ca^{2+}]. Hill coefficients for activation (n_H^a) varied from 0.8 to 5.2. Cardiac RyRs, in comparison, behaved more homogeneously. Most cardiac RyRs were closed at 100 nM [Ca^{2+}] and activated in a cooperative manner (n_H^a ranged from 1.6 to 5.0), reaching a high P_o (>0.6) in the presence and absence of Mg^{2+} and ATP. Heart RyRs were much less sensitive (10×) to inhibition by [Ca^{2+}] than skeletal RyRs. The differential heterogeneity of heart versus skeletal muscle RyRs may reflect the modulation required for calcium-induced calcium release versus depolarization-induced Ca^{2+} release.

INTRODUCTION

In skeletal muscle and heart, contraction is triggered by the rapid release of Ca^{2+} from the sarcoplasmic reticulum, which is mediated by the ryanodine receptor channels. The ryanodine receptors from skeletal and cardiac muscle (termed skeletal and cardiac RyRs, respectively) can be gated by Ca^{2+} as well as by a variety of diagnostic ligands (see reviews: Coronado et al., 1994; Dulhunty et al., 1996; Fleischer and Inui, 1989; Meissner, 1994; Ogawa, 1994; Sorrentino and Volpe, 1993).

Studies on the Ca^{2+} dependence of skeletal muscle and cardiac RyRs reconstituted into planar lipid bilayers differ in the estimate of cooperativity for Ca^{2+} activation, and on channel inhibition at millimolar [Ca^{2+}] (Ashley and Williams, 1990; Chu et al., 1993; Laver et al., 1995; Rousseau et al., 1992; Rousseau and Meissner, 1989; Sitsapesan and Williams, 1994; Smith et al., 1986). The apparent contradictions between reports have been attributed to differences in experimental conditions as well as to different types of muscle—that is, to the monovalent versus divalent ionic environments used as current carriers to study the channels, to different species, or to heterogeneity referable to different types of muscle (Chu et al., 1993; Coronado et al., 1994; Lee et al., 1991).

More recently, heterogeneous behavior of the channels was reported within muscle types in which one RyR isoform (RyR type I or RyR type II) predominates. Individual channels of the same preparation had different responses to ryanodine and ATP (Ma, 1995), millimolar [Ca^{2+}] (Laver et al., 1995), or ADP-ribose (Zahradníková et al., 1995). These studies suggested that heterogeneity may also be a consequence of differential modulation. In this regard, we found that for both skeletal muscle RyRs and cardiac RyRs, phosphorylation with protein kinases can overcome the block by Mg^{2+}, and again became sensitive to Mg^{2+}, when treated with protein phosphatases (Hain et al., 1994, 1995). Similarly, in heart SR, phosphorylation by CaM kinase II was found to overcome the block of cardiac RyRs by calmodulin (Witcher et al., 1991).

Heterogeneity of RyRs may be related to polypeptides that are associated with or bind to the channel. Calmodulin binds to skeletal RyRs and has two distinct effects. At nanomolar levels of cytosolic free [Ca^{2+}] ([Ca^{2+}]$_{free}$), it produced channel activation, whereas at μM [Ca^{2+}]$_{free}$, the addition of calmodulin inhibited the skeletal RyRs (Tripathy et al., 1995). Skeletal and cardiac RyRs are intimately associated with FK506 binding proteins, named FKBP12 and FKBP12.6, respectively, as heterooligomers (Timerman et al., 1993, 1994). FKBP12 has been demonstrated, by in vitro dissociation and reconstitution studies, to modulate the function of skeletal muscle RyR (Mayrleitner et al., 1994; Timerman et al., 1994) but not that of heart RyR (Barg et al., 1997; Timerman et al., 1996). The present study was designed to detect channel heterogeneity of skeletal and cardiac RyRs with regard to their response to cytosolic [Ca^{2+}]$_{free}$. We find that both rabbit skeletal muscle RyRs and dog heart RyRs behave as a heterogeneous population of channels. A preliminary report of this work has appeared (Copello et al., 1996).

MATERIALS AND METHODS

Drugs and chemicals

DibromoBAPTA (1,2-bis(2-amino-5-bromophenoxy)ethane-*N,N,N',N'*-tetraacetic acid) and HEDTA (*N*-(2-hydroxyethyl)ethylenediamine-

Received for publication 25 September 1996 and in final form 7 April 1997.

Address reprint requests to Prof. Sidney Fleischer, Department of Molecular Biology, Vanderbilt University, P.O. Box 1820, Station B, Nashville, TN 37235. Tel.: 615-322-2132; Fax: 615-343-6833; E-mail: fleiscs@ctrvax.vanderbilt.edu.

0006-3495/97/07/141/16 $2.00

N,N',N'-triacetic acid), obtained from Fluka (Buchs, Switzerland), were dissolved at 10–25 mM in aqueous buffer containing 50–125 mM Tris, and pH was titrated to 7.4 with HEPES. Phospholipids were obtained from Avanti (Alabaster, AL), and decane was from Aldrich (Milwaukee, WI). All other drugs and chemicals were from Sigma (St. Louis, MO) or were of reagent grade.

Isolation of membrane fractions

Skeletal muscle terminal cisternae fractions of sarcoplasmic reticulum were isolated from the predominantly white muscle of the leg and back of the rabbit as described by Saito et al. (1984). Sarcoplasmic reticulum (SR) fractions from canine heart were isolated as previously described (Chamberlain et al., 1983).

Bilayer technique

Planar lipid bilayers were formed on 110- or 180-μm-diameter circular holes in Teflon septa. The septa were tightly clamped with a metal ring between two half Teflon chambers, separating two 1.3-ml compartments that could be stirred with magnetic bars. The system has previously been described in detail (Schindler, 1989). The *cis* compartment was filled with a solution containing 250 mM HEPES and 120 mM Tris (pH 7.4). The *trans* compartment was filled with solution containing 250 mM HEPES and 53 mM $Ca(OH)_2$ (pH 7.4). Electrodes were Ag/AgCl pellets (Ref-2; Warner Instruments, Hamden, CT) immersed in 2 M KCl and connected to the chambers via 2 M KCl agar bridges. The *cis* solution was connected to ground. The *trans* solution potential was clamped by an EPC-7 patch-clamp amplifier (List Medical, Darmstadt, Germany). Membrane voltages (V_m) are reported with respect to the *trans* side of the chamber. Currents are depicted as negative (downward deflections) and denote cation flux from *trans* to *cis* compartments.

Bilayers of a 5:3:2 mixture of bovine brain phosphatidylethanolamine, phosphatidylserine, and phosphatidylcholine (50 mg/ml in decane) were painted onto the holes of bilayer septa from the *cis* side as previously described (Schindler, 1989). Bilayers utilized in our experiments had capacitances of 150–350 pF and leakage currents of less than 1 pA per 100 mV change in voltage.

After a 30-min period, to control bilayer stability, 500 mM CsCl and 1 mM $CaCl_2$ were added to the *cis* solution to facilitate fusion. Then 1–5 μg of protein of terminal cisternae vesicles from rabbit skeletal muscle or 2–10 μg of dog cardiac sarcoplasmic reticulum (SR) was added to the *cis* solution with stirring. In all cases the *cis* chamber was stirred until Cl^- currents were observed (usually within 1–5 min), and then the *cis* chamber was perfused at 3–4 ml/min with 20 ml of HEPES/Tris (250/120 mM, respectively, pH 7.4). The experiment was initiated only when channels with characteristics of the RyR were found (commonly one or two channels). That is, the channels identified as RyR had a current amplitude of 3.8–4.4 pA (skeletal RyRs) or 3.5–4.0 pA (cardiac RyRs) at 0 mV transmembrane voltage, a reversal potential of +40 mV (*trans* to *cis*), and a slope conductance of ~100 pS (skeletal RyRs) or 80 pS (cardiac RyRs).

RyR channels incorporate into the bilayers with their cytoplasmic face toward the *cis* chamber. Such channels are activated by *cis* (cytoplasmic) Ca^{2+} and/or ATP, and blocked by Mg^{2+}. When tested at the end of the experiments, the addition of ruthenium red (10 μM) to the *cis* chamber blocked the channels, and ryanodine (2 μM) locked the channels in a half-conductance open state. All of these responses are characteristics of RyR (Coronado et al., 1994; Dulhunty et al., 1996; Fleischer and Inui, 1989; Meissner, 1994; Ogawa, 1994). In our studies of calcium sensitivity of the RyR channels, we studied the effect of changing the free $[Ca^{2+}]$, defined as $[Ca^{2+}]_{cis}$, from nanomolar to millimolar ranges on the *cis* (cytoplasmic) side of the channel.

Single-channel currents were filtered at 500-1000 Hz with an eight-pole Bessel filter (Frequency Devices, Haverhill, MA) and digitized at 2–5 kHz using a Digidata 1200 analog-to-digital conversion system (Axon Instruments, Foster City, CA) for analysis by microcomputer. Data acquisition and analysis were carried out using the pClamp 6.03 program (Axon Instruments). Mean open probability (P_o) was determined for all conditions as the average of two to six segments of 20–180 s of channel recordings at each $[Ca^{2+}]_{cis}$ of the dose-response curves. In most cases, P_o was calculated by 50% threshold analysis. In recordings of channels having very short open times (some skeletal RyRs), in which the amplitudes are decreased by the filtering, or in experiments with multiple channels (number of channel current levels greater than five), P_o was also estimated as the proportion of areas in amplitude histograms. In multiple-channel experiments, the global open probability of all of the channels (nP_o values) was calculated. For simplicity of comparison with single-channel experiments, we show (in Figs. 1, 2, 8, 9, and 10) nP_o/x values, where x represents the number of current levels observed. This is likely to underestimate the total number of channels (n) in experiments with skeletal muscle RyR, because some channels had very low P_o at all Ca^{2+} concentrations. Substates were observed in ~30% of HA skeletal RyR channels when recordings were 20 min or longer, although their frequency compared with full opening was low (<1%). The amplitudes of the substates were 25%, 50%, and 75% of the full conductive opening. Conductance substates of 25% and 50% of the full channel conductance have also been observed with cardiac RyRs, but were rare; i.e., they were observed in less than 10% of the recordings and with low probability (the frequency of substates versus the frequency of full open events was lower than 0.2%). Consequently, the small contribution due to substates did not significantly affect the P_o. For studies of dwell-time distributions, segments with substates were not utilized.

Channel lifetimes were measured by half-amplitude threshold analysis of single-channel recordings of 2–4 min duration, filtered at 1 KHz, and digitized at 4–5 KHz. Openings and closings were binned every 400–500 ms and grouped into noncumulative histograms. A probability density function (PDF) = $\{a_1/\tau_1 \cdot \exp(-t/\tau_1) + \ldots a_i/\tau_i \cdot \exp(-t/\tau_i)\}$ containing $i = 1$ to 4 exponential terms (Colquhoun and Hawkes, 1995) was fitted to the histograms using the nonlinear regression curve routines of the program pStat 6.03 (Axon Instruments) and SigmaPlot 2.0 (Jandel Scientifics, Corte Madera, CA), which are both based on the Marquardt-Levenberg algorithm. τ_i are the closed or open time constants, and a_i are the fractional contribution of each component to the area under the curve ($\Sigma a_i = 1$). Fits were accepted only when all of the parameters were significantly different from zero. The number of exponential terms that best fit the histograms was determined according to both F test and the Akaike information criterion (Landaw and DiStefano, 1984). In addition to these criteria, the overlapping of the PDFs and the experimental data was also checked by eye. The analysis describes the characteristics of those events that are fully resolved by our bilayer system to compare differences between skeletal and cardiac RyR channels. Short-lived events (0–800 μs) were not considered for calculations. Parameters derived from the dwell-time histograms were not corrected for missed events. Not all individual channels exhibited the same number of time constants. Averages of time constants contain only τ_i values with area of distribution (a_i) different from zero. Average areas contain zeroes for those channels where fits do not include the respective time constant, to make the average $\Sigma a_i = 1$.

In our studies of Ca^{2+} sensitivity of the RyR channels, HEDTA (Bull and Marengo, 1993; Fabiato, 1988) or dibromoBAPTA (Harrison and Bers, 1987; Tsien, 1980) was utilized to effectively buffer free Ca^{2+}. The apparent dissociation constants (K_D) used for calculating $[Ca^{2+}]_{free}$, at pH 7.4 and 20°C for the Ca^{2+}-chelator complexes, are 2.2 μM for HEDTA, 1.8 μM for dibromoBATPA, and 0.06 μM for EGTA (Harrison and Bers, 1987, Fabiato, 1988). From these K_D values it is clear that both dibromoBAPTA and HEDTA buffer Ca^{2+} much more effectively than EGTA in the $[Ca^{2+}]_{cis}$ range of RyR activation (0.5–10 μM). Solutions of different free Ca^{2+} concentrations were prepared by mixing dibromoBAPTA with Ca^{2+} concentrations, as calculated by using stability constant values from Harrison and Bers (1987). For free Ca^{2+} concentrations in solutions prepared with HEDTA, calculations were made using the IONS program (Fabiato, 1988). First, 1 mM dibromoBAPTA (or HEDTA) was added to reduce Ca^{2+} levels to less than 50 nM (calculated assuming that residual Ca^{2+} in the solution was less than 20 μM). Then $CaCl_2$ or Ca-HEPES was added sequentially to achieve cumulative free $[Ca^{2+}]_{cis}$ of 100 nM to 10 mM. The addition of chelators and cumulative doses of calcium to the

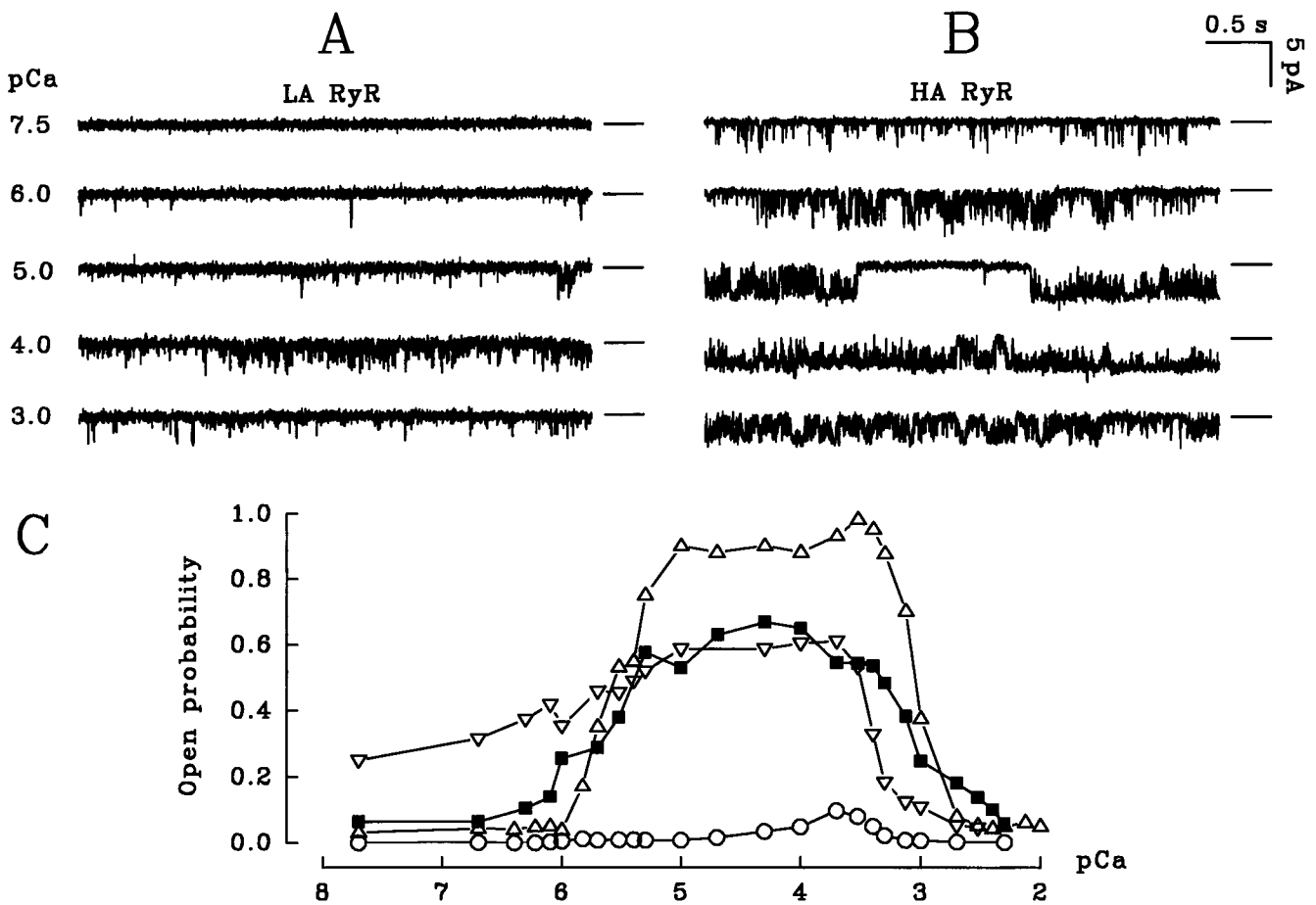

FIGURE 1 Gating by cytosolic Ca^{2+} ($[Ca^{2+}]_{cis}$) of ryanodine receptor channels from rabbit skeletal muscle terminal cisternae (skeletal RyRs). Skeletal RyRs were bathed in HEPES-Tris (cytosolic side) and HEPES/Ca^{2+} (luminal side); the holding potential was 0 mV. (*A*) Example of skeletal RyR Ca^{2+} currents by a low-activity channel (LA skeletal RyRs) at different pCa ($-\log [Ca^{2+}]_{cis}$); open events are shown as downward deflections. (*B*) Example of skeletal RyR Ca^{2+} currents by a high-activity channel (HA skeletal RyRs). (*C*) Single-channel P_o versus $[Ca^{2+}]_{cis}$. ○, Data points (each from 90-s recordings or longer) from a typical LA skeletal RyR; △ and ▽, data points from two high-activity (HA) skeletal RyR channels. nP_o/x data are from a multichannel experiment (■; x = 12 current levels observed).

bilayer chamber was done using graduated 10- and 50-μl syringes (Hamilton Company, Reno, NV) to minimize volumetric errors. The free $[Ca^{2+}]_{cis}$ levels were also confirmed by measuring the fluorescence of Fura2 in mixtures of various amounts of calcium and chelators as utilized in the experiments, or with a Ca^{2+} electrode.

For both skeletal and cardiac RyR channels, increasing $[Ca^{2+}]_{cis}$ to millimolar levels reduces the amplitude of the channel openings, as can be seen in Figs. 1 and 5. The relative permeability of Ca^{2+} versus Tris (P_{Ca}/P_{Tris}) is ~14 for RyR channels (for a review, see Coronado et al., 1994). Thus, increasing $[Ca^{2+}]_{cis}$ to millimolar levels reduced the driving force for net Ca^{2+} movements through the channel. In Fig. 1 we show currents at 1 mM Ca^{2+}, and in Fig. 5 currents at 5 mM (in this last case the driving force for Ca^{2+} movements at 0 mV is much lower). On average, current amplitudes decreased by ~15%, 30%, and 50% when $[Ca^{2+}]_{cis}$ increased from 10 μM to 1, 5, and 10 mM, respectively. Because high $[Ca^{2+}]_{cis}$ reduces channel conductance and perturbs the analysis, the $[Ca^{2+}]_{cis}$ was limited to 10 mM.

DibromoBAPTA was utilized in all of the experiments where 2 mM Mg^{2+} and 1 mM ATP (*cis* side) were present, because of its very low affinity for Mg^{2+} (K_D > 100 mM; Tsien, 1980). $[Ca^{2+}]_{cis}$ was not increased to millimolar levels in the presence of Mg^{2+} and ATP. Increasing $[Ca^{2+}]_{cis}$ to millimolar levels decreases the levels of free [ATP] (binding to Ca^{2+}) and increases the levels of free $[Mg^{2+}]$. Both Mg^{2+} and ATP are modulators of the channels (Coronado et. al., 1994; Meissner, 1994). Attempts to maintain free $[Mg^{2+}]$ and [ATP] at constant values necessitate changes in the levels of total $[Mg^{2+}]$ and [ATP], as well as added total $[Ca^{2+}]$, thereby introducing further variables. For this reason, our experiments tested only the effects of $[Ca^{2+}]_{cis}$ within a range in which, according to calculations from the IONS program (Fabiato, 1988), free and total levels of [ATP] and $[Mg^{2+}]$ did not change appreciably.

Statistics and curve fitting

Experimental values are expressed as means ± SEM. Curve fitting was done by nonlinear regression analysis of individual experiments and mean values, using commercially available programs based on the Marquardt-Levenberg algorithm (pClamp6, Axon Instruments; SigmaPlot 2.0, Jandel Scientific, Origin 3.0, MicroCal Software, Northampton, MA). In many experiments with skeletal and cardiac RyRs, the titration by $[Ca^{2+}]_{cis}$ was restricted to the phase of activation only, and in other experiments both the activation and inhibition phases were studied. To compare all experiments, we determined the parameters for the activation of RyRs with the Hill equation, $P_o = P_o^{ini} + ((P_o^{max} - P_o^{ini})/(1 + (EC_{50}/[Ca^{2+}]_{cis})^{n_H^a}))$. P_o^{ini} and P_o^{max} are the initial ($[Ca^{2+}]_{cis}$ < 50 nM) and maximum P_o values (average values at $[Ca^{2+}]_{cis}$ = 100 μM). EC_{50} is $[Ca^{2+}]_{cis}$ for half-maximum activation, and n_H^a is the Hill coefficient for the activation. For the phase of

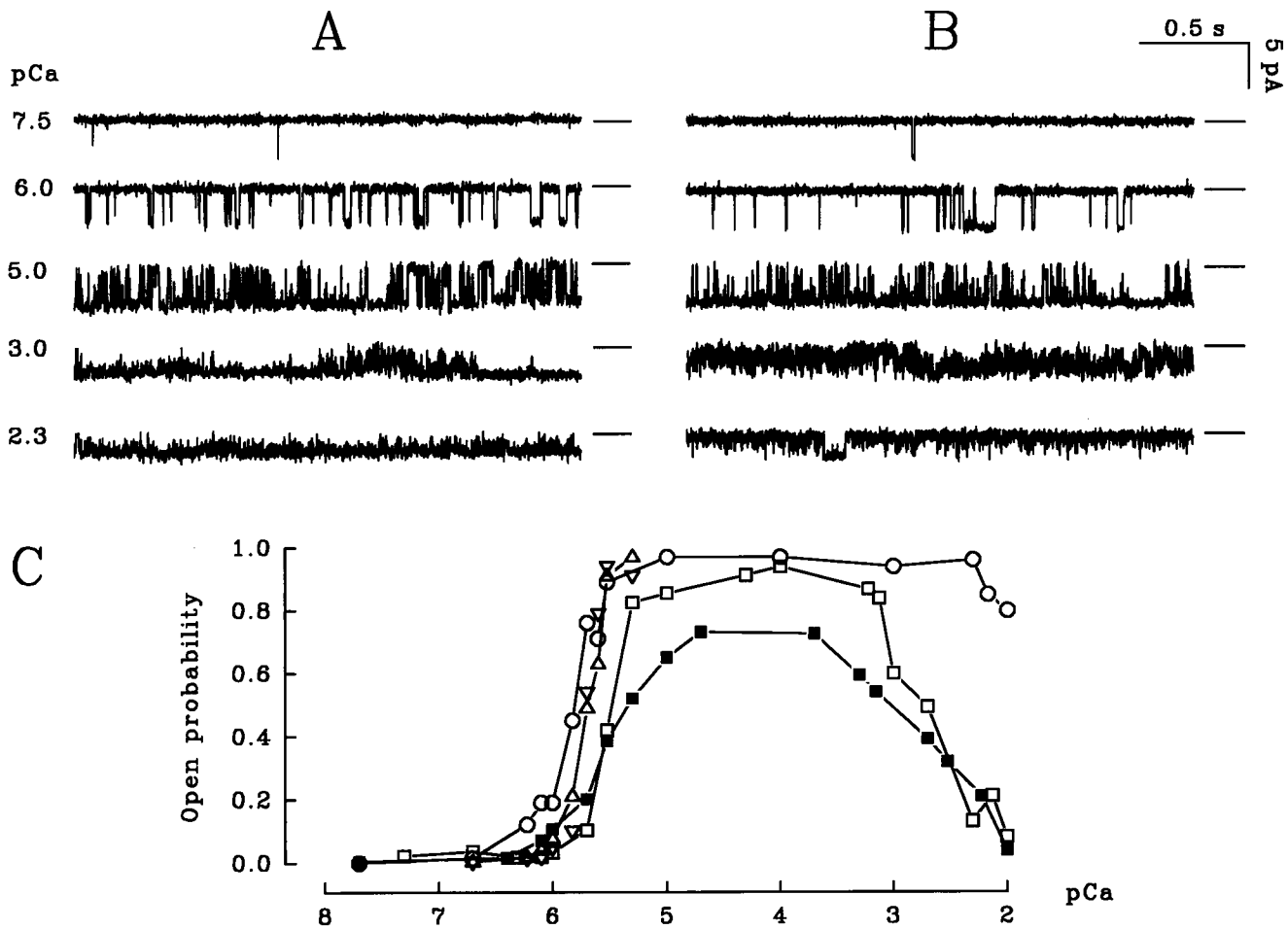

FIGURE 2 Gating by cytosolic Ca^{2+} of ryanodine receptor channels from dog cardiac muscle sarcoplasmic reticulum (cardiac RyRs). The experimental conditions were similar to those described in Fig. 1. (*A*) Example of Ca^{2+} currents as a function of $[Ca^{2+}]_{cis}$ from a cardiac RyR that is insensitive to inhibition by $[Ca^{2+}]_{cis} \leq 5$ mM. (*B*) As in *A*, for a cardiac RyR sensitive to inhibition by millimolar levels of Ca^{2+}. (*C*) P_o versus $[Ca^{2+}]_{cis}$ for two examples of single-channel behavior (○, □), and nP_o/x data for one multiple-channel experiment (■; $x = 4$ channels). ▽ and △, Duplicate P_o versus $[Ca^{2+}]_{cis}$ curves for a single channel obtained in two sequential runs, and between perfusions of the cytosolic bathing solution with HEPES/Tris.

inhibition of the RyRs by $[Ca^{2+}]_{cis}$, we used the equation $P_o = P_o^{res} + (P_o^{max} - P_o^{res})/[1 + ([Ca^{2+}]_{cis}/EC_{50})^{n_H^i}]$, where P_o^{res} and P_o^{max} are residual (fraction of P_o insensitive to inhibition by $[Ca^{2+}]_{cis}$) and maximum P_o values at $[Ca^{2+}]_{cis} = 100$ μM. IC_{50} is the $[Ca^{2+}]_{cis}$ for the half-maximum inhibitory effect (IC_{50}), and n_H^i is the Hill coefficient for the inhibition.

RESULTS

Skeletal muscle RyRs show extremes of behavior with regard to calcium gating, whereas cardiac RyRs behave more homogeneously

Sarcoplasmic reticulum vesicles from rabbit skeletal or dog cardiac muscle were incorporated into planar lipid bilayers, and the effects of varying cytosolic free Ca^{2+} ($[Ca^{2+}]_{cis}$) on the open probability (P_o) of a large number of ryanodine receptors from skeletal and cardiac muscle were studied.

Skeletal muscle RyR channels show a wide variation of activity under comparable conditions, indicating a heterogeneous population. This is exemplified in Fig. 1, which shows extremes of the response to $[Ca^{2+}]_{cis}$. For simplification, we classify them as low-activity (LA) and high-activity (HA) skeletal RyR, despite the fact that a range of intermediate behaviors was also found within the second group.

Low-activity channels (LA skeletal RyR) are defined as channels that were almost inactive or had little activity in the $[Ca^{2+}]_{cis}$ range of 50 nM to 10 mM. As shown in the example of Fig. 1, *A* and *C* (*open circles*), openings of LA skeletal RyRs at low $[Ca^{2+}]_{cis}$ (nanomolar) were scarce ($P_o < 0.01$) and brief (a few milliseconds). The frequency of openings increased with $[Ca^{2+}]_{cis}$ from 20 nM to 100–200 μM, where P_o reached maximum values of ~0.1. The channel activity decreased to low levels at higher $[Ca^{2+}]_{cis}$ (millimolar) (Fig. 1, *A* and *C*). Most of these channels had such a biphasic response to $[Ca^{2+}]_{cis}$, albeit with overall low activity. The example shown in Fig. 1, *A* and *C* (*open circles*) is representative for 6 out of 20 experiments with skeletal muscle RyRs. One additional channel studied always had $P_o < 0.02$ and was therefore also classified as LA,

even though it did not have a clear biphasic response to $[Ca^{2+}]_{cis}$ (not shown). Thus skeletal LA RyRs as defined above were found in ~35% of the single-channel experiments (7 of 20 experiments here, and 4 of 14 in the presence of Mg^{2+} and ATP; see later).

High-activity channels (HA skeletal RyRs) resemble skeletal RyRs as reported by a number of laboratories (Coronado et al., 1994; Dulhunty et al., 1996). Example current traces of HA skeletal RyRs are shown in Fig. 1 *B*, recorded at several $[Ca^{2+}]_{cis}$ (pCa ranged from 7.5 to 3.0). Fig. 1 *C* plots P_o values versus $[Ca^{2+}]_{cis}$ for two examples of single channels and one experiment with several channels simultaneously present in the bilayer. HA skeletal RyRs displayed a biphasic response to $[Ca^{2+}]_{cis}$, with high variability in the observed open probability at all $[Ca^{2+}]_{cis}$. HA skeletal RyRs reached maximum P_o values of 0.60 ± 0.14 (ranging from 0.18 to 0.96, n = 13).

Cardiac ryanodine receptor (cardiac RyR) channel recordings at $[Ca^{2+}]_{cis}$ ranging from 100 nM to 5 mM are shown in Fig. 2, *A* and *B*. Cardiac RyRs also displayed a biphasic response to $[Ca^{2+}]_{cis}$. They reached maximum P_o values of 0.82 ± 0.11 (ranging from 0.36 to 0.99, n = 12). Most of the channels were closed at $[Ca^{2+}]_{cis} < 0.1$ μM, and became fully activated with 10 μM $[Ca^{2+}]_{cis}$, as illustrated in the examples. (Fig. 2 *C*). Inhibition of the channels required millimolar $[Ca^{2+}]_{cis}$.

Populational analysis reveals high variability in the calcium sensitivity of skeletal, but not cardiac, RyRs

To assess the degree of heterogeneity and the population differences among cardiac and skeletal RyRs, P_o values of many individual RyR channels were compared at three $[Ca^{2+}]_{cis}$, defined as "low" (<50 nM for skeletal, 100 nM for cardiac RyRs), "mid" (reflecting the peak P_o value, e.g., between 20 and 200 μM), and "high" (1 mM). In one set of experiments, we evaluate the $[Ca^{2+}]_{cis}$ activation of the channels from "low" to "mid" $[Ca^{2+}]_{cis}$ (Fig. 3, *C* and *D*)

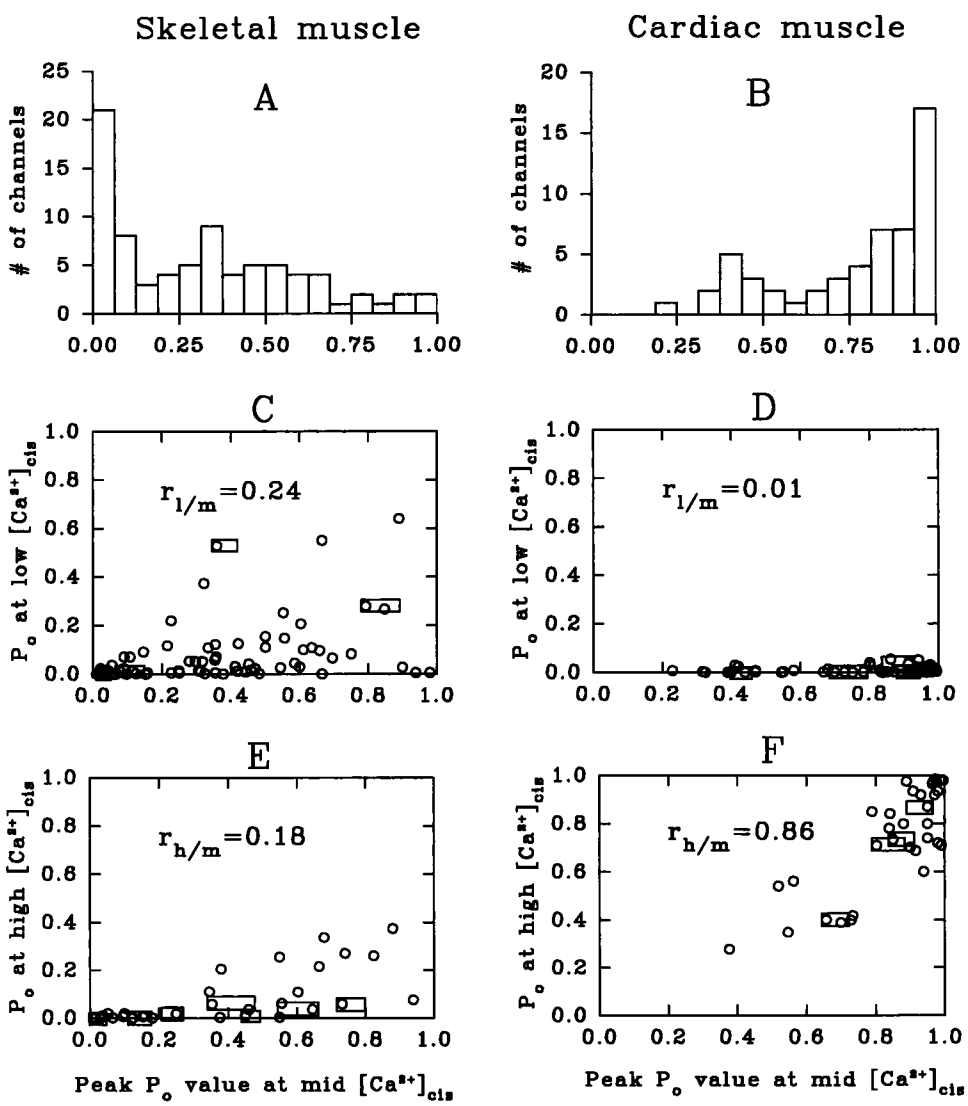

FIGURE 3 Comparison of P_o values of skeletal RyRs (*A*, *C*, *E*) and cardiac RyRs (*B*, *D*, *F*) at three $[Ca^{2+}]_{cis}$ levels. The *x* axes (from *A* to *F*) always represent the peak P_o values of individual channels found at midrange $[Ca^{2+}]_{cis}$ (midrange was at 10–200 μM). *A* and *B* show frequency of distribution of P_o values (no. of channels) found at mid-$[Ca^{2+}]_{cis}$ for 80 skeletal RyRs (*A*) and for 55 cardiac RyRs (*B*). P_o values were grouped using intervals of 0.065 units of P_o. (*C* and *D*) Comparison of P_o values at low $[Ca^{2+}]_{cis}$ as a function of paired P_o values at mid-$[Ca^{2+}]_{cis}$ (low concentrations were $[Ca^{2+}]_{cis} < 50$ nM for skeletal RyRs, and $[Ca^{2+}]_{cis}$ = 100 nM for cardiac RyRs). Also shown in the figures, the ratio of P_o values between low and mid-$[Ca^{2+}]_{cis}$ ($r_{l/m}$) for skeletal and cardiac RyRs, respectively. (*E* and *F*) Comparison of P_o values at high $[Ca^{2+}]_{cis}$ as a function of paired P_o values at mid-$[Ca^{2+}]_{cis}$ (high concentration is $[Ca^{2+}]_{cis}$ = 1 mM for both cardiac and skeletal RyRs). The ratio of P_o values between high and mid-$[Ca^{2+}]_{cis}$ ($r_{h/m}$) for skeletal and cardiac RyRs is also indicated in the figures. The boxes in *C*, *D*, *E*, and *F* show the range of variations found between the first and a duplicate determination of P_o at mid-$[Ca^{2+}]_{cis}$.

and, in a second set, at "mid" and "high" $[Ca^{2+}]_{cis}$ (Fig. 3, *E* and *F*), the inhibition of RyRs by $[Ca^{2+}]_{cis}$. Individual P_o values at "low" and "high" $[Ca^{2+}]_{cis}$, respectively, were plotted against P_o values of the same channel at "mid" $[Ca^{2+}]_{cis}$ (the distribution of "mid" P_o values is given in Fig. 3, *A* and *B*, respectively).

The differences in behavior of the skeletal RyRs as compared with cardiac RyRs are dramatic. Both groups of channels show (at least) bimodal distribution of peak P_o values (Fig. 3, *A* and *B*). Skeletal RyRs were found to have peak P_o values at "mid" $[Ca^{2+}]_{cis}$ from near 0 to 1 (Fig. 3 *A*). For cardiac RyRs, the peak P_o values estimated at "mid" $[Ca^{2+}]_{cis}$ (in the range between 20 and 100 μM) varied less (Fig. 3 *B*). Most of the skeletal RyR channels ($n = 80$) had $P_o < 0.5$ (Fig. 3 *A*), whereas most of the cardiac RyRs ($n = 55$) reached $P_o \approx 0.5$ or higher (Fig. 3 *B*). Consequently, the peak P_o values of cardiac RyRs averaged to 0.750 ± 0.033, higher ($p < 0.01$) than 0.326 ± 0.030 for skeletal RyRs. At "low" $[Ca^{2+}]_{cis}$, nearly 30% of skeletal RyRs had $P_o < 0.01$; the remaining 70% had P_o between 0.01 and 0.6 (Fig. 3 *C*). Most of the cardiac RyRs were silent ($P_o < 0.01$) at "low" $[Ca^{2+}]_{cis}$; values of $P_o > 0.05$ were rare (Fig. 3 *D*). The mean P_o value for skeletal RyRs was 0.073 ± 0.016 at "low" $[Ca^{2+}]_{cis}$. For cardiac RyRs, it was less (0.011 ± 0.002; $p < 0.01$), even though $[Ca^{2+}]_{cis}$ was buffered at somewhat higher levels (Fig. 3 legend). The mean ratio of P_o values "low" versus "mid" $[Ca^{2+}]_{cis}$ ($r_{l/m}$) was 0.240 ± 0.028 for skeletal RyRs, much higher ($p < 0.01$) than $r_{l/m} = 0.014 \pm 0.003$ for cardiac RyRs.

Fig. 3 *E* shows paired P_o values of skeletal RyRs at mid versus high $[Ca^{2+}]_{cis}$. The response of skeletal RyRs to millimolar $[Ca^{2+}]_{cis}$ was heterogeneous, with 40% retaining considerable activity, yet the other 60% was practically closed. The mean P_o value of the channels greatly decreased from 0.360 ± 0.081 at mid $[Ca^{2+}]_{cis}$ to 0.083 ± 0.041 at high $[Ca^{2+}]_{cis}$ ($n = 33$, paired observations). Fig. 3 *F* shows that cardiac RyRs were less sensitive to inhibition by $[Ca^{2+}]_{cis}$. At high $[Ca^{2+}]_{cis}$ the mean P_o was 0.741 ± 0.039, compared with 0.848 ± 0.029 for mid $[Ca^{2+}]_{cis}$ ($n = 33$). The mean ratio of P_o values at high versus mid $[Ca^{2+}]_{cis}$ ($r_{h/m}$) was 0.18 ± 0.04 for skeletal RyRs, much less than for cardiac RyRs ($r_{h/m} = 0.86 \pm 0.03$, $p < 0.01$). Thus the decrease in P_o of cardiac RyRs was only ~14%, much less than the 82% observed with skeletal RyRs ($p < 0.01$).

Fig. 3 illustrates evidence for the presence of at least two groups of channels in skeletal muscle. P_o values at mid $[Ca^{2+}]_{cis}$ varied widely; however, the frequency of channels with low P_o (range 0.01–0.13) was more than twice that of channels with higher P_o (Fig. 3 *A*). In addition, most of the channels with $P_o < 0.1$ had very low activity at low (Fig. 3 *C*) and high $[Ca^{2+}]_{cis}$ (Fig. 3 *E*), whereas most of the active channels showed variable activity at both low and high $[Ca^{2+}]_{cis}$. This notion enables us to sharpen our definition of LA skeletal RyRs. LA channels have very low activity at low and high $[Ca^{2+}]_{cis}$, and reach a maximum $P_o < 0.1$ at mid $[Ca^{2+}]_{cis}$ of ~100–200 μM. On the other hand, it becomes clear that HA skeletal RyRs represent a wide range of channel behavior.

Heterogeneity in channel behavior is not due to experimental error in the determination of P_o

To estimate the error of P_o, duplicate determinations were performed on the same channel by perfusing the *cis* chamber with HEPES/Tris (see Materials and Methods), and then reestablishing the experimental conditions of the initial set of measurements (by adding the same amount of dibromoBAPTA/calcium). Ranges of variation between original and duplicate values of peak P_o values are given as boxes in Fig. 3, *C* and *E*, for skeletal RyRs and Fig. 3, *D* and *F*, for cardiac RyRs. For the same skeletal RyR channels, the average difference between two P_o determinations (first minus repeat) was 0.06 ± 0.01 (the range was from 0.01 to 0.13; $n = 11$ experiments). For the 11 channels tested, the mean P_o value was 0.352 ± 0.088, and P_o values ranged from 0.02 to 0.90. Thus the range of variability between two measurements from the same channel was only 15% of the variation among P_o values of different channels. Likewise, the P_o determinations for cardiac RyRs were reasonably reproducible (Fig. 3, *D* and *F*). Similar reproducibility was found also at other $[Ca^{2+}]_{cis}$ for both cardiac and skeletal RyRs (not shown), and for titrations of $[Ca^{2+}]_{cis}$ (shown for cardiac RyRs in Fig. 2 *C*, *upright open triangles* and *inverted open triangles* for first and second run, respectively). It can be concluded that the wide ranges of channel behavior observed in skeletal and cardiac RyR populations reflect mainly heterogeneity among individual channels, rather than experimental error.

Open and closed time distribution varies widely among skeletal, but not cardiac, RyRs

The diary plot (P_o versus time) of a LA skeletal RyR (as defined above), recorded with 100 μM $[Ca^{2+}]_{cis}$ (Fig. 4 *A*), shows that channel activity was low most of the time; i.e., there were no bursts of high open probability. In most cases, this pattern was consistently observed during prolonged experiments (>40 min). For this LA RyR channel, short openings (<5 ms) predominated, as shown in the open time histogram (Fig. 4 *B*). Open events had time constants (τ_1 and τ_2) of 1.18 ms (93% of the area of distribution) and 5.4 ms (7%). The closed event histogram of this channel (Fig. 4 *C*) shows only 22% short closures ($\tau_1 = 2.00$ ms), 34% with $\tau_2 = 9.82$ ms and 44% with $\tau_3 = 54.2$ ms. Similar values were found for the open and closed time constants of six other channels, all recorded in 100 μM $[Ca^{2+}]_{cis}$ (see Fig. 2 legend). Thus the low P_o value of LA RyR results from the predominance of short openings and long closures.

For one example of HA skeletal RyR (Fig. 5 *A*) with 100 μM $[Ca^{2+}]_{cis}$, the diary plot shows that P_o oscillated between low and high values. The open time distribution of this HA skeletal RyR shows predominantly short events

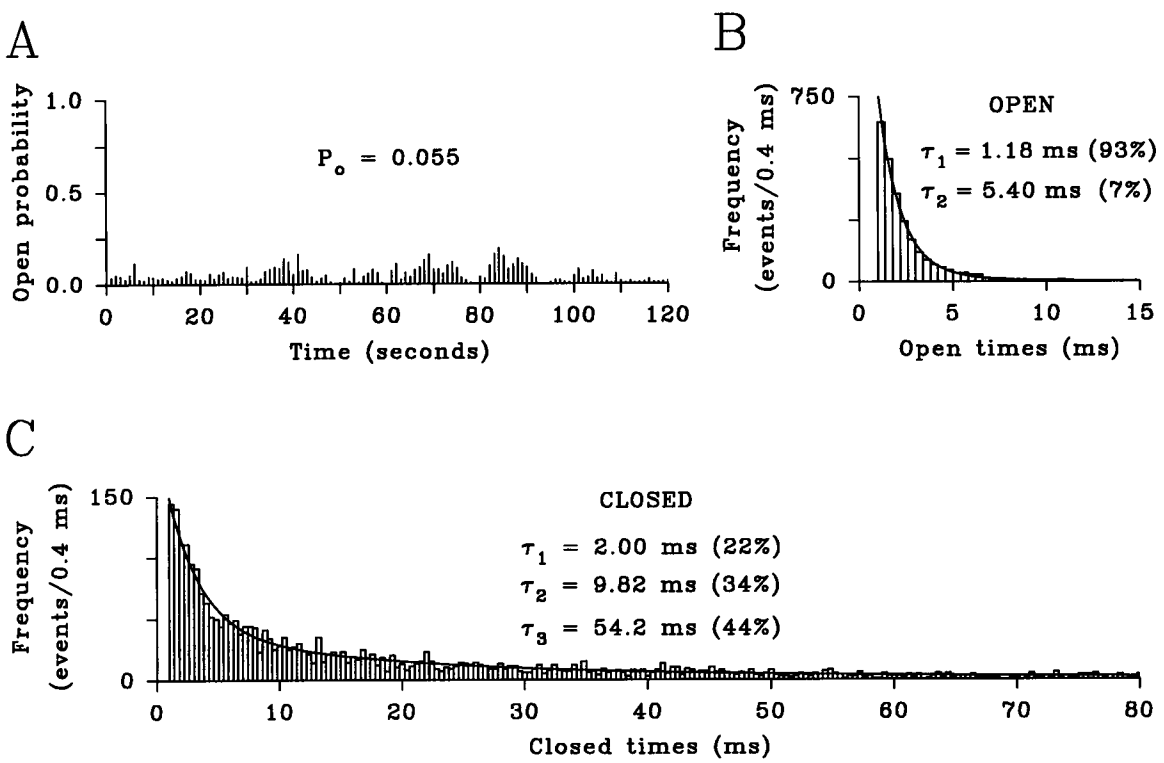

FIGURE 4 Gating of a LA skeletal RyR at 0 mV and with 100 μM $[Ca^{2+}]_{cis}$. (*A*) Open probability (P_o) estimated in consecutive segments of 1 s (*bars*). Note that the activity is low during the entire record length (120 s); the mean average P_o for the whole trace was 0.055. (*B*) Open lifetime histograms were constructed for resolved openings of the LA skeletal RyRs (*bars*; bin size of 0.4 ms), and the probability density function (PDF, *solid line*) was estimated by nonlinear regression analysis (see Materials and Methods). (*C*) Closed lifetime distributions (*bars*) and PDF (*solid line*). The time constants (τ_i) for open- and closed-time histograms and their respective areas (given in parenthesis as %; $\Sigma a_i\% = 100$), obtained by fitting the PDFs to the dwell-time distributions, are shown in *B* and *C*, respectively. Typical histograms are shown in this figure. The average parameters for seven LA skeletal RyRs at 100 μM $[Ca^{2+}]_{cis}$ were as follows. Open times: τ_1 = 0.97 ± 0.11 ms (range from 0.80 to 1.29 ms), a_1 = 93 ± 2% (87–100%), τ_2 = 3.94 ± 0.58 ms (2.70–5.91 ms), a_2 = 7 ± 2% (0–13%). Closed times: τ_1 = 1.30 ± 0.20 ms (range from 0.82 to 2.00 ms), a_1 = 27 ± 5% (12–55%), τ_2 = 7.61 ± 0.93 ms (3.69–11.20 ms), a_2 = 33 ± 2% (27–42%), τ_3 = 57.1 ± 8.9 ms (37.0–97.9 ms), a_3 = 40 ± 4% (19–53%).

(Fig. 5 *B*), yet the fit to the data required three exponential terms. The time constants, τ_1 and τ_2, of 0.94 ms (66% of the area) and 3.45 ms (24%) had a range similar to that found for LA channels. This HA channel also had openings distributing with a longer time constant (τ_3 = 16 ms), which was not observed for the LA RyR channels. More importantly, the closures were mostly short (Fig. 5 *C*), with time constants of 1.1 ms (71%) and 6.14 ms (29%). Time distributions similar to those in Fig. 5, *B* and *C*, were seen in nine other HA channels (with 100 μM $[Ca^{2+}]_{cis}$; average values are given in Fig. 5 legend). As a consequence of shorter closures, the frequency of openings and the P_o values are greater in HA skeletal RyRs compared with LA RyRs. Closed time distributions with a significant amount of long closures were found in HA skeletal RyR, only with submaximally activating $[Ca^{2+}]_{cis}$ (1–2 μM, not shown).

Cardiac RyRs exposed to 100 μM $[Ca^{2+}]_{cis}$ usually had high P_o, as shown in the example of Fig. 6 *A*. The open time distribution of this cardiac RyR (Fig. 6 *B*) was fitted with three exponential terms, and time constants of 1.2, 7.9, and 24.7 ms. The average τ_3 of this and nine other experiments were significantly higher than for HA skeletal RyR channels ($p < 0.05$; Fig. 6 legend). Long openings prevailed in cardiac RyRs, as indicated by the distribution area of each time constant (Fig. 6 *B*, and legend of Fig. 6), in contrast with HA skeletal RyR, where shorter events were much more frequent (Fig. 5 *B* and legend of Fig. 5). The closed time distribution of cardiac RyRs was similar to that of HA skeletal RyRs, containing mostly short events (Fig. 6 *C*, and Fig. 6 legend). As a consequence of a higher frequency of long open events and fewer substates (see Materials and Methods), traces from cardiac RyR channel recordings (Fig. 2, *A* and *B*, and Fig. 10) usually showed better resolved gating events than the traces from skeletal RyRs (Figs. 1 and 9).

Parameters of activation/inhibition by calcium are different in skeletal versus cardiac RyRs

$[Ca^{2+}]_{cis}$ titration curves of single skeletal and cardiac RyRs channels, similar to those already shown in Figs. 1 and 2, were analyzed for parameters of $[Ca^{2+}]_{cis}$ activation and inhibition.

For skeletal LA RyRs (as defined above), the approximate estimation of parameters was done without curve

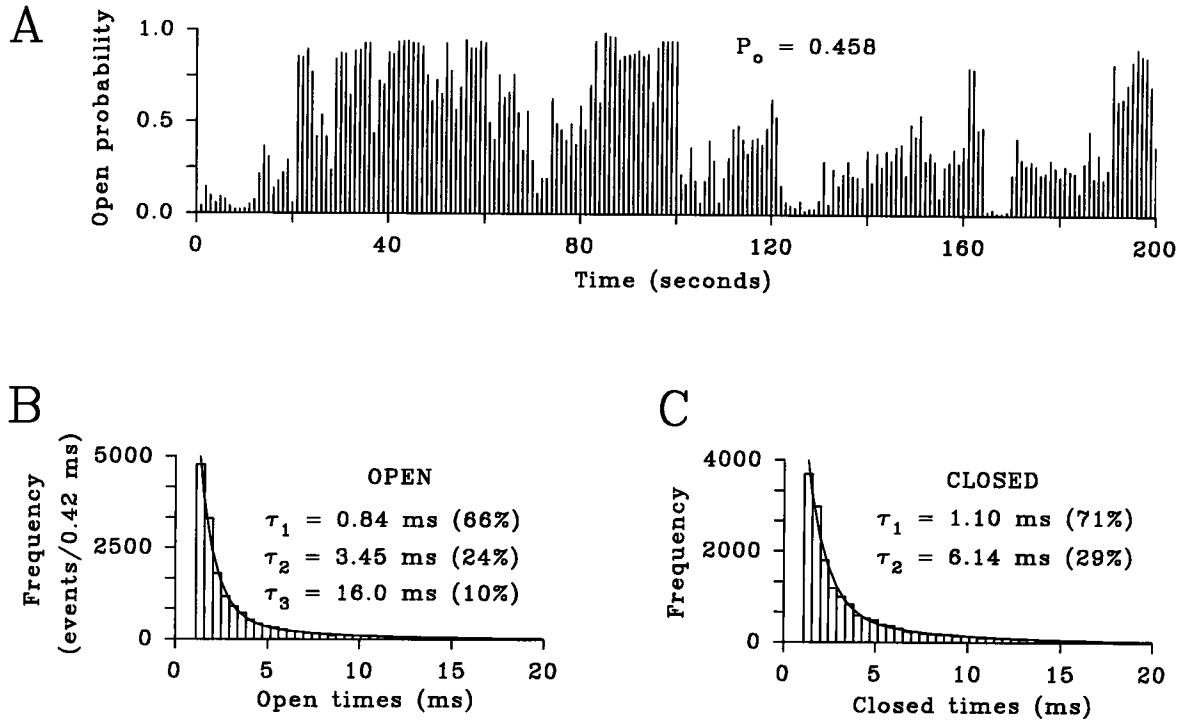

FIGURE 5 Gating of a HA skeletal RyRs at 0 mV and with 100 μM $[Ca^{2+}]_{cis}$. (*A*) Open probability (P_o) estimated in consecutive segments of 1 s (*bars*). Note that there are periods of variable activity (low and high). The mean average of P_o for the whole trace of 200 s was 0.458. (*B*) Open lifetime histograms (*bars*; bin size of 0.44 ms) and probability density function (PDF, *solid line*). (*C*) Closed lifetime distributions (*bars*) and PDF (*solid line*). The time constants (τ_i) and areas (as % in parenthesis) are shown. The average values of these parameters for this example and nine other skeletal RyR channels in 100 μM $[Ca^{2+}]_{cis}$ were as follows. Open times: τ_1 = 0.94 ± 0.08 ms (range from 0.80 to 1.60 ms), a_1 = 61 ± 4% (36–86%), τ_2 = 4.24 ± 0.50 ms (2.74–7.20 ms), a_2 = 29 ± 3% (14–40%), τ_3 = 20.1 ± 3.2 ms (10.6–36.7 ms), a_3 = 10 ± 3% (0–30%). Closed times: τ_1 = 0.90 ± 0.12 ms (range from 0.60 to 1.25 ms), a_1 = 82 ± 2% (71–91%), τ_2 = 3.87 ± 0.58 ms (1.60–6.13 ms), a_2 = 18 ± 2% (9–29%).

fitting, because the low P_o precludes the use of fitting algorithms. For six experiments in which the activation phase was clearly identified, $[Ca^{2+}]_{cis}$ for half-maximum activation (EC_{50}) was ~70 to 150 μM. The $[Ca^{2+}]_{cis}$ for half-maximum inhibitory effect (IC_{50}) was in the range of 100–300 μM (n = 5).

HA skeletal RyRs activated with EC_{50}'s almost one order of magnitude lower than the range EC_{50}'s estimated for LA RyRs. We observed a high degree of variation in the shape of the P_o versus $[Ca^{2+}]_{cis}$ curves as well as in EC_{50}'s, with the latter ranging from 0.7 to 8.9 μM $[Ca^{2+}]_{cis}$ (Fig. 7 *A*, *open circles*). Note that EC_{50}'s within this range were observed with all HA channels, even when peak P_o values were as low as 0.18. Seven out of 13 HA skeletal RyRs activated with Hill coefficients (n_H^a) greater than 1, four others had $n_H^a \approx 1$ (see examples given in Fig. 1 *C*, *upright and inverted open triangles*). In two additional cases, P_o at 50 nM $[Ca^{2+}]_{cis}$ was ≥0.4, and no clear $[Ca^{2+}]_{cis}$ dependence was observed (not shown). Mean values for the data in Fig. 7 *A* were EC_{50} = 3.1 ± 0.7 μM (range from 0.7 to 8.9 μM) and n_H^a = 2.6 ± 0.5 (range from 0.8 to 5.0).

The IC_{50} for $[Ca^{2+}]_{cis}$ and the Hill coefficient for the inhibition (n_H^i) of four single HA skeletal RyRs are shown in Fig. 7 *B* (*open circles*). There was a sevenfold variation in IC_{50}'s (range 0.16–1.1 mM). The n_H^i of individual skeletal RyRs also varied, ranging from 2 to 5.1, indicative of high cooperativity for the inhibition of the channels by Ca^{2+}. Mean values were IC_{50} = 0.50 ± 0.21 mM and n_H^i = 3.7 ± 0.7.

In single cardiac RyR channel experiments, we observed differences in their individual n_H^a and EC_{50}, and in the peak P_o values of the $[Ca^{2+}]_{cis}$ curves (compare *open circles* and *open squares* in Fig. 2 *C*). Kinetic parameters for 12 single cardiac RyRs are given in Fig. 7 *A* (*open circles*). The individual EC_{50}'s varied between 1 and 5 μM, and had $n_H^a \approx$ 2–5. The latter is in contrast with HA skeletal RyRs, in which cooperativity on the activation by $[Ca^{2+}]_{cis}$ was observed in just half of the channels.

Cardiac RyRs were less sensitive to inhibition by millimolar $[Ca^{2+}]_{cis}$ than skeletal RyRs. Fig. 2, *A* and *C*, shows a typical example of five similar cardiac RyRs channels, where P_o was unaffected by increasing $[Ca^{2+}]_{cis}$ up to 5 mM (*open circles*); a small decrease in P_o was observed at higher $[Ca^{2+}]_{cis}$ (≥ 7.5 mM). However, in seven other experiments, P_o decreased continuously as the $[Ca^{2+}]_{cis}$ was increased, and approached zero (see examples in Fig. 2, *B* and *C*, *open circles*). Thus there is heterogeneity with respect to $[Ca^{2+}]_{cis}$ inhibition. The individual IC_{50} and n_H^i for the seven "inhibitable" cardiac RyRs channels are shown in Fig. 7 *B*; mean values were IC_{50} = 5.3 ± 1.1 mM (range

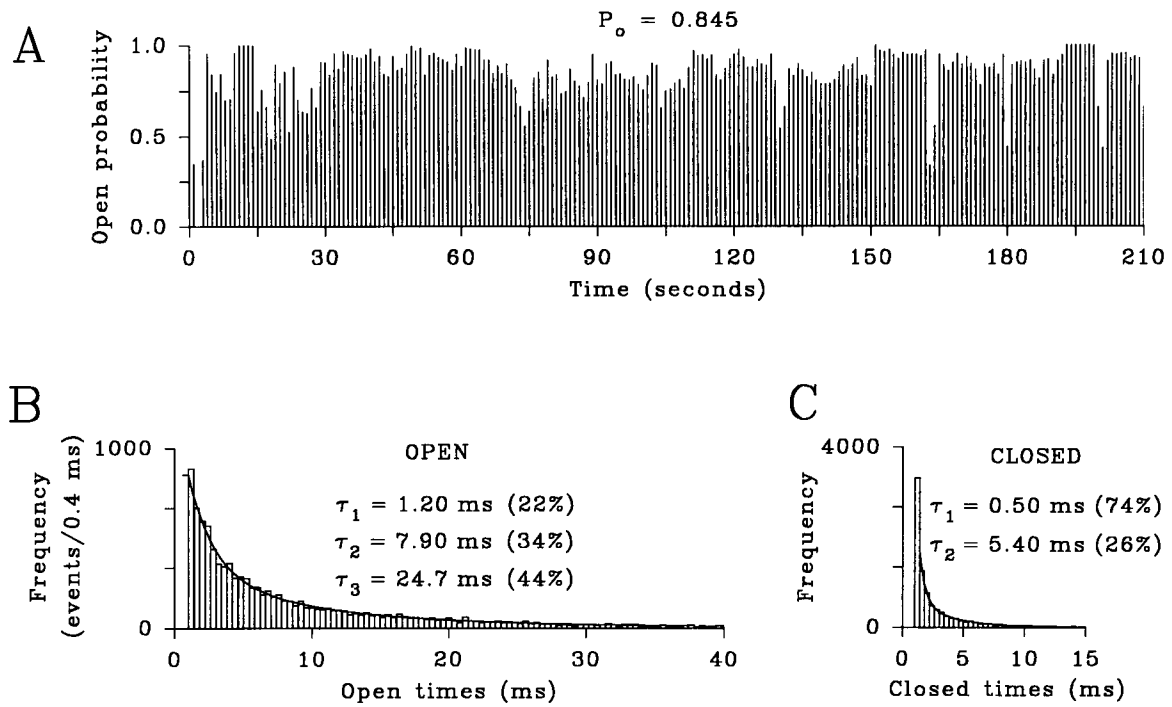

FIGURE 6 Gating of a dog cardiac RyR at 0 mV and with 100 μM $[Ca^{2+}]_{cis}$. (*A*) Open probability (P_o) estimated in consecutive segments of 1 s (*bars*). Note that high values of P_o predominate; the average P_o for the whole record (210 s) was 0.845. (*B*) Open-lifetime histograms (*bars*; bin size of 0.4 ms) and probability density function (PDF, *solid line*). (*C*) Closed-lifetime distributions (*bars*) and PDF (*solid line*). The time constants (τ_i) and areas (as % in parenthesis) are shown. The average values of these parameters for this example and nine other cardiac RyR channels at 100 μM $[Ca^{2+}]_{cis}$ were as follows. Open times: τ_1 = 0.84 ± 0.08 ms (range from 0.40 to 1.10 ms), a_1 = 31 ± 6%* (15–66%), τ_2 = 6.68 ± 1.30 ms (2.90–11.20 ms), a_2 = 29 ± 4% (12–43%), τ_3 = 43.0 ± 7.9 ms* (15.3–81.6 ms), a_3 = 40 ± 7%* (17–62%) (*values were significantly different from those of HA skeletal RyRs; $p < 0.05$ or better). Closed times: τ_1 = 0.68 ± 0.07 ms (range from 0.37 to 1.14 ms), a_1 = 73 ± 5% (52–100%), τ_2 = 3.07 ± 0.37 ms (1.60–7.30 ms), a_2 = 27 ± 6% (0–48%).

2.0–8.1 mM), and n_H^i = 2.6 ± 0.7. Not all cardiac RyRs were inhibited cooperatively; the range of n_H^i was 1.2–3.7 (Fig. 7 *B*). Note that the average of the IC_{50}'s for the "inhibitable" cardiac RyRs (5.3 mM) was roughly 10 times higher than for HA skeletal RyRs (0.50 mM), even though for the $[Ca^{2+}]_{cis}$ activation, the EC_{50}'s were comparable (Fig. 7, *A* and *B*).

Results from multichannel records can be explained as average of LA and HA skeletal RyRs

In almost half of all successful reconstitutions of RyRs into planar lipid bilayers, more than one active channel is observed. Such experiments were disregarded above, to simplify the analyses. However, the majority of channels were

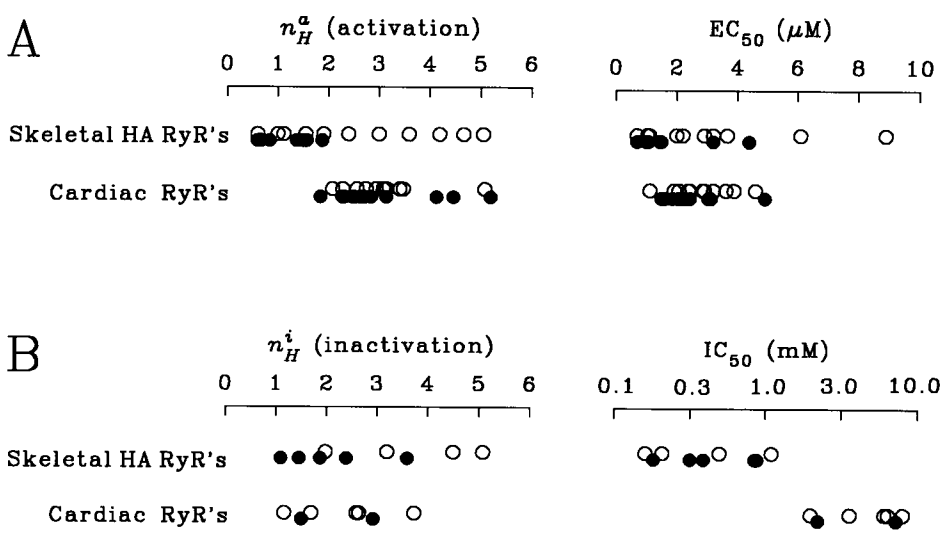

FIGURE 7 Comparison of parameters of single versus multiple RyR channels for the activation and inhibition by $[Ca^{2+}]_{cis}$. (*A*) EC_{50} and n_H^a of the activation of HA skeletal RyRs and cardiac RyRs as a function of $[Ca^{2+}]_{cis}$. Individual values of single-channel experiments (○) and multiple-channel experiments (●). (*B*) IC_{50} and n_H^i of the inhibition of HA skeletal RyRs and cardiac RyRs as a function of $[Ca^{2+}]_{cis}$. Individual values of single-channel experiments (○) and multiple-channel experiments (●). In five other experiments, IC_{50} of cardiac RyRs appear to be higher than the upper limits of $[Ca^{2+}]_{cis}$ tested.

observed in multichannel experiments. Therefore, we studied whether multiple channel records behave like the averaged population of individual channels.

An example of a multichannel experiment with skeletal muscle RyRs is shown in Fig. 1 *C* (*filled squares*). Similar to this, biphasic responses to $[Ca^{2+}]_{cis}$ were observed in six other experiments (estimated to contain 4–12 current levels). The estimated parameters for each experiment are given in Fig. 7 *A* (*filled circles*). The average of the EC_{50}'s was 1.91 ± 0.52 μM, which is comparable to that of HA skeletal RyRs (3.1 ± 0.7 μM). Mean n_H^a was 1.04 ± 0.21, considerably lower than that of single HA skeletal RyRs (2.6 ± 0.5). As expected, channels that have very little activity (e.g., LA RyR) do not contribute significantly to changes in nP_o. Thus the parameters will reflect mainly HA skeletal RyRs. The finding that $n_H^a \approx 1$ is likely due to averaging of data from single channels with different EC_{50}'s.

Fig. 8 illustrates this phenomenon. The summation of all HA skeletal RyR (*open circles*) single-channel data results in a titration curve very similar to that obtained from the summation of all multichannel experiments (*open squares*). n_H^a (= 1.3) is much lower than in individual experiments (n_H^a = 2.6). When LA RyR data are added to the summation (HA + LA channels; *inverted open triangles*), the EC_{50}'s and n_H^a are not significantly changed. However, the plateau P_o values are now decreased by one-third.

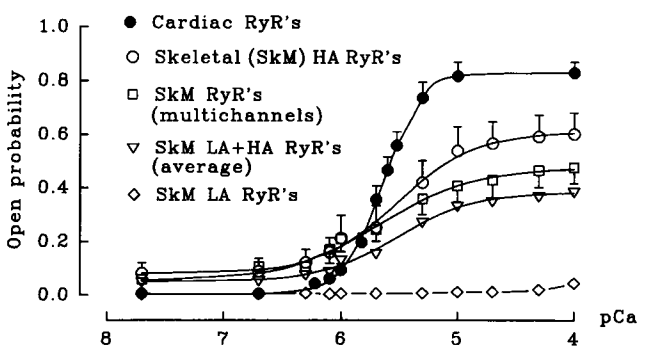

FIGURE 8 Comparison of the activation by $[Ca^{2+}]_{cis}$ of skeletal and cardiac RyRs. For skeletal muscle, skeletal RyR averaged values of P_o versus $[Ca^{2+}]_{cis}$ are presented for single HA skeletal RyR channels (○; n = 11), for the LA skeletal RyR channels (◇, n = 7), for all single (HA + LA) skeletal RyR channels (▽ n = 18), and for multichannel experiments (□, n = 7). For cardiac muscle, in which no important differences were observed between single- and multiple-channel experiments, the average of all $[Ca^{2+}]_{cis}$ activation curves with cardiac RyRs (●; n = 24) is shown. The solid lines represent the fit to the data of the Hill equation for $Ca^{2+}]_{cis}$ activation: $P_o = P_o^{ini} + ((P_o^{max} - P_o^{ini})/(1 + (EC_{50}/[Ca^{2+}]_{cis})^{n^a_H}))$. P_o^{ini} and P_o^{max} are initial (low $[Ca^{2+}]_{cis}$<5 nM) and maximum values of P_o ($[Ca^{2+}]_{cis}$ = 100 μM) determined experimentally; EC_{50} and n^a_H have their usual meanings. For HA skeletal RyRs, values are P_o^{ini} = 0.09, P_o^{max} = 0.60, EC_{50} = 2.9 μM, and n_H^a = 1.3. For LA skeletal RyR channels, no parameters were determined by curve fitting. For HA + LA channel experiments, P_o^{ini} = 0.05, P_o^{max} = 0.40, EC_{50} = 2.3 μM, and n_H^a = 1.1. For multi-skeletal RyR channel experiments, P_o^{ini} = 0.055, P_o^{max} = 0.44, EC_{50} = 2.2 μM, and n_H^a = 1.1 (values were very close to the average of HA + LA channels). For the pooled cardiac RyRs, values are P_o^{ini} = 0.01, P_o^{max} = 0.84, EC_{50} = 2.3 μM, and n_H^a = 2.6. Note that only the range of $[Ca^{2+}]_{cis}$ (from 50 nM to 100 μM), where these channels activated (and not the inhibition phase), is displayed.

The parameters for 12 multiple channel experiments with cardiac RyRs (Fig. 7 *A*, *filled circles*; two to five channels per bilayer) did not differ significantly from those of single-channel experiments, indicating homogeneous behavior; the mean n_H^a was 2.9 ± 0.2 (range 1.8–4.5), and the mean EC_{50} was 2.4 ± 0.3 μM (range 1.5–5.0 μM). Pooled data of all cardiac RyR experiments (single and multichannel) are plotted in Fig. 8 (*filled circles*). The n_H^a = 2.6 for the pooled average indicates that cardiac RyR's activate over a narrower range of $[Ca^{2+}]_{cis}$ than skeletal RyR.

In a similar manner, we found comparable parameters for the inhibition phase in single channel versus multichannel experiments (Fig. 7 *B*, *filled circles*) for both skeletal and cardiac RyRs. For five multichannel skeletal RyR experiments, we estimated mean IC_{50} = 0.52 ± 0.14 mM (range 0.18–0.8 mM) and mean n_H^i = 2.0 ± 0.4 (range 1.1–3.0). Two multichannel experiments with cardiac RyRs had n_H^i's and IC_{50}'s comparable to those of single channels (Fig. 7 *B*).

We conclude that multichannel experiments reflect the average behavior of single channels. However, such multichannel experiments mask the presence of different populations of individual channels.

LA skeletal RyRs are RyRs

The gating of LA skeletal RyRs is quite different from that of HA skeletal RyRs, although the two channel types have similar current amplitudes at 0 mV (in the range of 3.6–4.3), similar slope conductances (80–100 pS), and reversal potentials (~40 mV *cis* minus *trans* potential). LA RyRs had responses similar to those of diagnostic ligands as described for RyRs in general (Coronado et al., 1994; Fleischer and Inui, 1989; Meissner, 1994; Ogawa, 1994): LA skeletal RyRs were reversibly blocked by 1 mM Mg^{2+} (n = 10/10). ATP (2 mM) reversibly activated the channels (no Mg^{2+} present, $[Ca^{2+}]_{cis}$ < 50 nM); e.g., P_o increased from values of near zero (range 0–0.003) to 0.15 ± 0.04 (range 0.05–0.28, n = 6). Ryanodine (1 μM; n = 3) induced very long openings of about one-third the normal current amplitudes, well established effects of this drug on skeletal and cardiac RyRs. Finally, in a small percentage of experiments (~7%), LA and HA types were observed to spontaneously interconvert. The irreversible switch from HA to LA was observed five times, and the opposite was observed twice, i.e., from LA to HA skeletal RyR.

Heterogeneity of RyRs is also observed in the presence of Mg^{2+} and ATP

Both ATP and Mg^{2+}, normally present in the cytosol, modulate RyR channels (Coronado et al., 1994; Meissner, 1994; Ogawa, 1994). We therefore studied RyR channel heterogeneity in the presence of Mg^{2+} (total 2 mM, free $[Mg^{2+}] \approx$ 1 mM) and ATP (total 1 mM).

The range of $[Ca^{2+}]_{cis}$ in our experiments was chosen to study the activation of RyRs, while keeping nearly constant the levels of total and free concentrations of both Mg^{2+} and ATP (see Materials and Methods).

A diversity of responses was observed for skeletal muscle RyRs. In six of 14 experiments, the channels had very low activity ($P_o \leq 0.01$) over the whole range of $[Ca^{2+}]_{cis}$ studied (50 nM to 50 μM), as shown for an example in Fig. 9, *A* and *C* (*open circles*). In two of these cases, the channel behaved like HA skeletal RyRs, both before addition and after removal of ATP and Mg^{2+}. Thus the lack of activity in the presence of ATP and Mg^{2+} was not due simply to channel inactivation. In four other cases, channels had the characteristics of LA skeletal RyRs before and after the addition of ATP and Mg^{2+}.

In the remaining eight experiments, the channels were activated by increasing $[Ca^{2+}]_{cis}$ from 50 nM to 50 μM. As in the absence of Mg^{2+} and ATP (Fig. 1 *C*), heterogeneity among individual channels was observed (Fig. 9, *B* and *C*). The shape of the P_o versus $[Ca^{2+}]_{cis}$ curves varied, as shown for two extreme examples (*upright and inverted open triangles*) of seven individual channels, and a multichannel experiment (*filled squares*) in Fig. 9 *C*. The parameters for the activation by $[Ca^{2+}]_{cis}$ are given in Fig. 11 *A*. Both the mean of the EC_{50}'s (3.2 ± 0.7 μM; range 1.1–7.0 μM) and the mean of the n_H^a's (3.3 ± 0.6; range 1.2–5.2) were similar to those in the absence of Mg^{2+} and ATP (3.1 μM and 2.6, respectively).

Titrations of $[Ca^{2+}]_{cis}$ were not pursued beyond 100 μM, to avoid other complicating effects of millimolar $[Ca^{2+}]_{cis}$. Nevertheless, decreased skeletal RyR channel activity was observed with $[Ca^{2+}]_{cis} > 1$ mM ($n = 3$). Such high $[Ca^{2+}]_{cis}$ results in changes of free $[Mg^{2+}]$ (increase) and free [ATP] (decrease), which complicate the interpretation.

Cardiac RyRs had a homogeneous response to $[Ca^{2+}]_{cis}$, when studied in the presence of 2 mM Mg^{2+} and 1 mM ATP (Fig. 10). The channels were closed at $[Ca^{2+}]_{cis} < 1$ μM, activated in the micromolar range, and reached an activation plateau at $[Ca^{2+}]_{cis}$ = 20–200 μM (200 μM values not shown in Fig. 11). Individual EC_{50}'s and n_H^a's showed some scatter (Fig. 11 *A*). The mean EC_{50} (16.4 ± 2.6 μM; range from 1.6–2.6 μM) was higher than in the absence of ATP and Mg^{2+} (3.1 μM, $p < 0.01$), whereas the

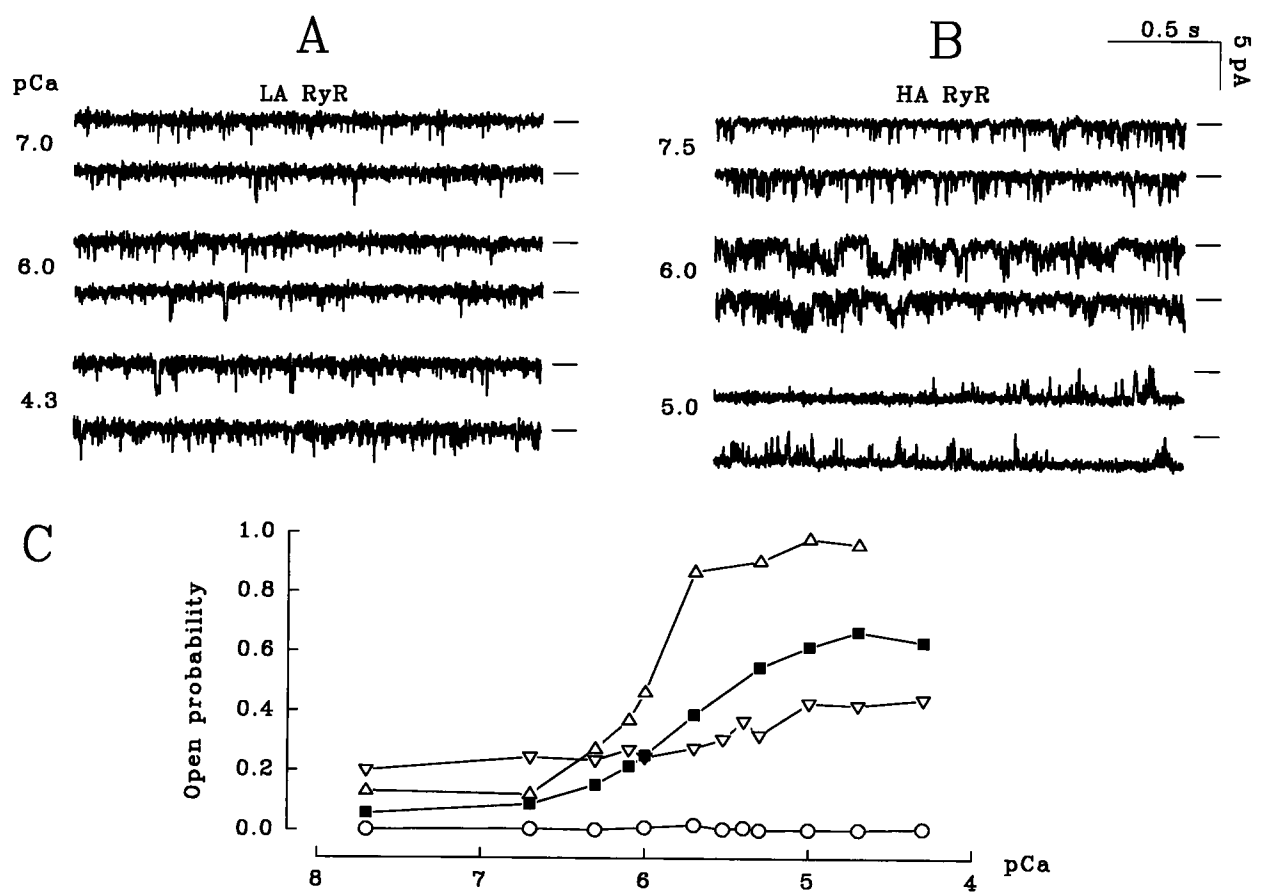

FIGURE 9 Activation by $[Ca^{2+}]_{cis}$ of skeletal RyRs in the presence of Mg^{2+} and ATP. Conditions are similar to those in Fig. 1, except that 2 mM Mg^{2+} and 1 mM ATP were added to the cytosolic solutions. (*A*) Example of skeletal RyR Ca^{2+} currents from a low-activity channel (LA skeletal RyRs). (*B*) Ca^{2+} currents from a high-activity channel (HA skeletal RyRs). (*C*) Single-channel P_o versus $[Ca^{2+}]_{cis}$. Data points from a LA skeletal RyR (○). Data points from two high-activity (HA) skeletal RyR channels (△ and ▽). Clearly, LA and HA channels display different patterns of Ca^{2+} activation. nP_o/x data from a multichannel experiment (■; $x = 5$ current levels observed).

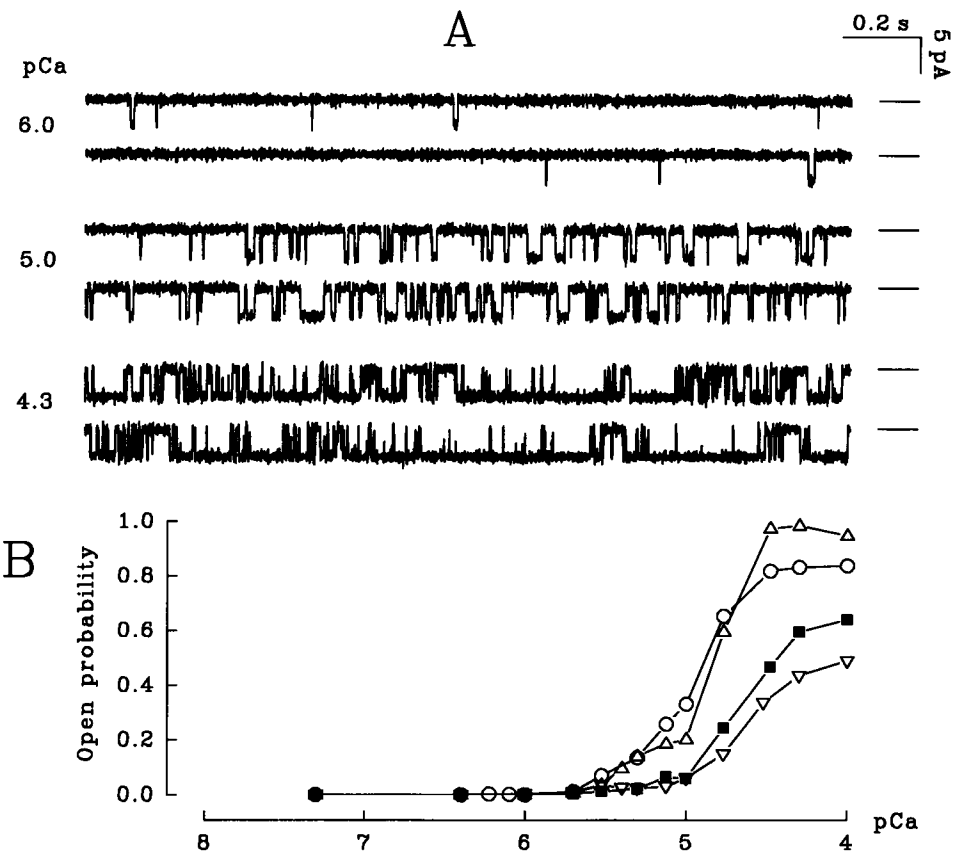

FIGURE 10 Activation by $[Ca^{2+}]_{cis}$ of cardiac RyRs in the presence of 2 mM Mg^{2+} and 1 mM ATP. (*A*) Example of recordings of cardiac RyR channel currents at different $[Ca^{2+}]_{cis}$. (*B*) Examples of single-channel P_o versus $[Ca^{2+}]_{cis}$ data for three single-channel experiments (○, △, ▽) and nP_o/x of one multiple-channel experiment (■, x = two current levels observed). The channels differed in EC_{50}'s and with regard to plateau values of P_o.

mean n_H^a (2.1 ± 0.2; range 1.6–2.6) was slightly lower, perhaps indicative of decreased cooperativity.

Comparison of the averaged data for those single HA skeletal RyRs remaining active with Mg^{2+} and ATP (seven of nine) and all RyRs is shown in Fig. 11 *B*. Averaged cardiac RyRs had higher EC_{50}, but similar n_H^a and maximum P_o values compared with averaged HA (Fig. 11 *B* legend). For pooled HA skeletal RyRs, n_H^a's were similar in the absence or presence of Mg and ATP (1.3 and 1.5), but lower than the averaged n_H^a's of individual HA skeletal RyRs channels (3.1 and 3.3, respectively). As described earlier, this is a consequence of heterogeneous behavior of HA skeletal RyRs. Cardiac RyRs channels were again more homogeneous than HA skeletal RyRs (compare parameters in Fig. 11 *A*); therefore the n_H^a of the averaged data was similar to the mean n_H^a of individual channels (1.75 and 2.1, respectively).

DISCUSSION

This study documents the functional heterogeneity of calcium release channels from sarcoplasmic reticulum of skeletal muscle and heart with regard to gating by cytosolic Ca^{2+}. Heterogeneity, much more pronounced for skeletal RyRs, was observed in both the absence and presence of Mg^{2+} and ATP, which was largely referable to differences in behavior of the channels and not to experimental error. The data reveal important differences between the RyRs of skeletal and cardiac muscle. In the following, some interesting aspects of our findings are discussed.

Differences in the Ca^{2+} gating of skeletal versus cardiac RyRs

A key finding of this study is the identification and characterization of a distinct group of low-activity (LA) RyR channels in skeletal muscle, which can be readily discerned from all other skeletal RyRs that were classified as HA skeletal RyRs. Comparable observations have been reported in RyRs from rat brain microsomes (Marengo et al., 1996), and with purified α-RyR of chicken skeletal muscle (Percival et al., 1994). No equivalent for LA RyRs was found in heart in any of the studies. LA and HA channel behaviors appear to represent separate gating modes of the same channel protein, as suggested by spontaneous irreversible switches between them (reported here), and the finding that changes in the gating of rabbit skeletal muscle RyR can be induced by applying voltage pulses (Ma, 1995). Evidence for such an interconversion of gating modes was also found in experiments with purified chicken RyR-α (Percival et al., 1994), where ~25% of the channels reversibly switched between behaviors resembling the LA and HA types defined here. It seems unlikely therefore that LA RyRs are just decayed versions of "typical" (HA) channels; they appear to

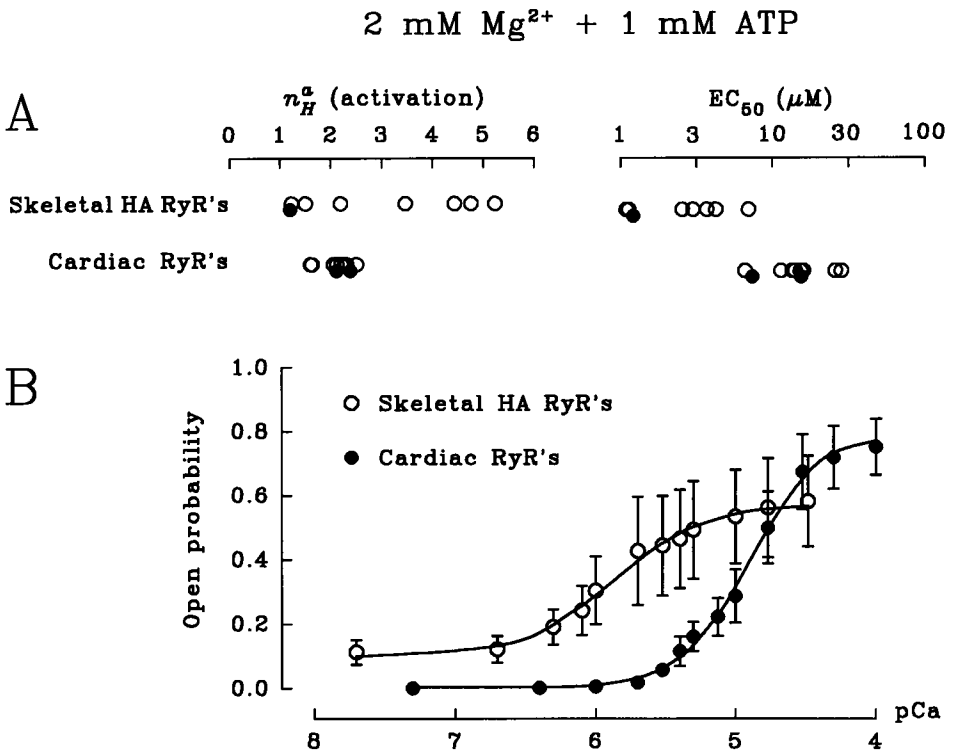

FIGURE 11 Comparison of the activation by $[Ca^{2+}]_{cis}$ of skeletal and cardiac RyRs in the presence of 2 mM Mg^{2+} and 1 mM ATP. (*A*) EC_{50} and n_H^a of the activation of HA skeletal RyRs and cardiac RyRs as a function of $[Ca^{2+}]_{cis}$. Individual values of single-channel experiments (○) and multiple-channel experiments (●). (*B*) Comparison of the activation by $[Ca^{2+}]_{cis}$ of average HA skeletal RyRs and cardiac RyRs. Averaged P_o versus $[Ca^{2+}]_{cis}$ curves of seven experiments with single HA skeletal RyRs, where Ca^{2+} activation was observed (○), and of 10 experiments with cardiac RyRs (●). The solid lines represent the fit of the Hill equation to the data (see Fig. 9 legend). For skeletal RyRs, values are $P_o^{ini} = 0.10 \pm 0.01$, $P_o^{max} = 0.56 \pm 0.14$, $EC_{50} = 2.9 \pm 0.2$ μM, and $n_H^a = 1.5 \pm 0.1$. For cardiac RyRs, values are $P_o^{ini} = 0.00 \pm 0.00$*, $P_o^{max} = 0.74 \pm 0.10$, $EC_{50} = 13.0 \pm 1.0$ μM*, and $n_H^a = 1.8 \pm 0.1$ (*skeletal RyR and cardiac RyR values are significantly different; $p < 0.01$).

be, instead, a "special" gating mode of skeletal RyRs. Indeed, bursting behavior of skeletal and cardiac RyRs with alternating periods of low and high P_o was recently demonstrated (Armisén et al., 1996; Zahradníková and Zahradník, 1995). In this context, LA skeletal RyRs could be interpreted as RyRs locked in the low P_o bursting mode.

Additional differences between skeletal muscle and heart were observed. HA skeletal RyRs displayed a wide variation in 1) P_o values at low $[Ca^{2+}]_{cis}$, 2) peak P_o values at mid $[Ca^{2+}]_{cis}$, 3) parameters of activation by $[Ca^{2+}]_{cis}$, and 4) inhibition at high $[Ca^{2+}]_{cis}$. For skeletal muscle, the presence of several channel types in addition to LA was observed, which could not be resolved from the continuum of channel behavior. With the exception of inhibition by high (millimolar) $[Ca^{2+}]_{cis}$, such pronounced heterogeneity was not observed in heart. Most cardiac RyRs were closed at $[Ca^{2+}]_{cis} < 0.1$ μM, activated in a cooperative manner, and reached high peak P_o values (>0.6). Cardiac RyRs were much less sensitive to the inhibition by $[Ca^{2+}]_{cis}$, requiring 1–10 mM $[Ca^{2+}]_{cis}$ to observe a significant decrease in activity.

HA skeletal and cardiac RyRs gave similar mean EC_{50}'s, but the cardiac RyRs activated in a narrower range of $[Ca^{2+}]_{cis}$, and from much lower to much higher P_o values. LA skeletal RyRs activated with EC_{50}'s at least an order of magnitude higher than HA skeletal RyRs and cardiac RyRs. In conclusion, the response to $[Ca^{2+}]_{cis}$ of skeletal RyRs is more graded than that of cardiac RyRs. Activation of cardiac RyRs in the presence of Mg^{2+} and ATP required much higher $[Ca^{2+}]_{cis}$ than in the absence of these two agents (mean EC_{50}'s 16.4 μM versus 2.8 μM). This was not the case for skeletal HA RyRs (mean EC_{50}'s 3.2 μM versus 3.1 μM) and may be related, at least in part, to the effects of physiological modulation by ATP (Coronado et al., 1994). It would therefore be of interest to assess the effect of pharmacological agents in the presence of physiological concentrations of Mg^{2+} and ATP.

Comparison with previous reports

Heterogeneity

The presence of LA RyR channels seems to have been overlooked in studies on mammalian skeletal muscle (Smith et al., 1986; Rousseau et al., 1992; Chu et al., 1993; Coronado et al., 1994). Only recently, two distinct channel populations were found in purified α-RyR from chicken skeletal muscle (Percival et al., 1994). Two other reports suggest a heterogeneous $[Ca^{2+}]_{cis}$ modulation of channels with characteristics like those of HA skeletal RyRs in rabbit skeletal muscle and sheep heart (Laver et al., 1995). Our study is the only one that we are aware of that compares $[Ca^{2+}]_{cis}$ activation in the presence of Mg^{2+} and ATP for skeletal and cardiac RyRs.

Cooperativity of calcium activation

We consistently found high cooperativity for the activation of heart RyRs by $[Ca^{2+}]_{cis}$. Our data are in agreement with earlier reports ($n_H^a \approx 2$–4) for sheep cardiac RyRs (Laver et al., 1995; Sitsapesan and Williams, 1994), but contrast with $n_H^a \approx 1$ found in other reports (Ashley and Williams, 1990;

Chu et al., 1993; Rousseau and Meissner, 1989). Most of our skeletal RyRs were cooperatively activated, although the n_H^a's ranged from 0.8 to 5.2. Our data are in contrast to previously reported values ($n_H^a \leq 1$) for rabbit skeletal RyRs (Chu et al., 1993; Laver et al., 1995; Rousseau et al., 1992), and for RyR from nonmammalian skeletal muscle (Bull and Marengo, 1993; Percival et al., 1994; O'Brien et al., 1995). Such apparent discrepancies may reflect, at least in part, heterogeneity of the skeletal and cardiac RyR populations. As demonstrated in the Results, the use of multiple channels or averaged P_o values from pooled data could have affected calculations of n_H^a's, because of marked differences in individual channels of the EC_{50}'s for $[Ca^{2+}]_{cis}$. The most credible n_H^a values for the cooperativity of skeletal RyRs are those from individual single-channel experiments.

Inhibition at millimolar calcium

This is the first report that rabbit skeletal RyRs and dog cardiac RyRs are biphasically gated by cytosolic Ca^{2+} when calcium is used as the charge carrier. The response to $[Ca^{2+}]_{cis}$ described here resembles data obtained using ryanodine binding and calcium flux as assays for channel function (Chamberlain et al., 1984; Chu et al., 1993; Fabiato, 1983; Meissner, 1984; Nagasaki and Kasai, 1983; Pessah et al., 1985). Inhibition of skeletal muscle RyR from several species by millimolar cytosolic Ca^{2+} was observed in bilayer experiments, only when monovalent ions were used as charge carriers (Chu et al., 1993; Laver et al., 1995; Percival et al., 1994; O'Brien et al., 1995; but see Bull and Marengo, 1993), but not with high *trans* $[Ca^{2+}]$ (Rousseau et al., 1992; Smith et al., 1986). This discrepancy has been attributed to the modulatory effects of high luminal $[Ca^{2+}]$ on the RyRs (Coronado et al., 1994), which is not tenable, in view of our results.

We also find inhibition of cardiac RyRs, although at very high $[Ca^{2+}]_{cis}$. This contrasts with a number of previous studies (Chu et al., 1993; Rousseau and Meissner, 1989; Ashley and Williams, 1990; Sitsapesan and Williams, 1994). Recently, cardiac RyRs were inhibited within a similar range of $[Ca^{2+}]_{cis}$, when Cs^+ (*trans*) was used as the charge carrier (Laver et al., 1995). Thus it seems possible that $[Ca^{2+}]_{cis}$ used in many of these studies may not have been high enough for inhibition. As biphasic $[Ca^{2+}]_{cis}$ responses were also reported for RyRs from various other nonmuscular tissues, as well as for inositol(1,4,5)triphosphate receptors (IP3R) (Bezprozvanny et al., 1991; Marengo et al., 1996), inhibition by high $[Ca^{2+}]_{cis}$ emerges as a general property of calcium release channels.

Speculations on the molecular basis of channel heterogeneity

The observed functional heterogeneity in heart and skeletal muscle does not appear to be referable to a significant heterogeneity of RyR isoforms in these tissues. The ryanodine receptor isoforms I and II (RyR1 and RyR2) predominate (>95%) in skeletal and cardiac muscle, respectively. The level of RyR3 expression in fast twitch skeletal muscle fibers is small (several percent or less) and not readily detectable in cardiac myocytes (Coronado et al., 1994; Dulhunty et al., 1996; Ogawa, 1994; Sorrentino and Volpe, 1993). However, regions for alternative splicing have recently been identified in RyRs as possible sources of two RyR mRNA transcripts found in skeletal muscle, which could lead to functionally different channels from a single gene (Zorzato et al., 1994).

Considering the complex modulation of RyR channels characterized mainly by in vitro studies, we should expect to find a heterogeneous population of RyRs. Some of the mechanisms that could explain heterogeneity include reversible covalent modifications, such as phosphorylation/dephosphorylation events (Witcher et al., 1991; Hain et al., 1994, 1995). Furthermore, ryanodine receptors can be modulated by associated proteins. Removal of the FK-506 binding protein FKBP12 reversibly increases the sensitivity of skeletal muscle RyRs to calcium and other ligands (Mayrleitner et al., 1994; Timerman et al., 1994). We estimated that a small percentage of the channels may be devoid of FKBP12 (Timerman et al., 1995), and some may be further lost upon incorporation into the bilayer. Thus the loss of FKBP in some channels may also explain, in part, the heterogeneity of skeletal RyR channels. In cardiac tissue, the removal of FKBP12.6 has no apparent functional effect (Barg et al., 1997), which suggests different physiological roles in excitation-contraction (EC) coupling, and may underlie, at least in part, differences in the heterogeneity of RyRs in cardiac versus skeletal muscle. Other associated peptides (Coronado et al., 1994; Dulhunty et al., 1996) that have been reported to modulate RyRs are calmodulin (Tripathy et al., 1995) and sorcin (Lokuta et al., 1997).

Differences between the characteristics of skeletal RyRs have previously been related to distinct functions of different types of muscle, as between "slow twitch" and "fast twitch" muscle (Lee et al., 1991). Similarly, the finding of heterogeneous populations of skeletal RyRs in predominantly "white" muscle from rabbit (this report, Laver et al., 1995), chicken (Percival et al., 1994), fish (O'Brien et al., 1995), and frog (Bull and Marengo, 1993) could be related to dissimilar fibers within the same muscle type. However, heterogeneity of channels also occurs within a single skeletal muscle fiber, as indicated by the observation of heterogeneity of calcium release events among individual triads of frog skeletal muscle (Blatter et al., 1996).

Differential association of the channels with other proteins may also underlie the observed heterogeneity. At the transverse tubule-sarcoplasmic reticulum junctions (triads), RyRs (foot structures) are arranged in orderly arrays at the junctional face membrane of terminal cisternae, as shown by electron microscopy (Franzini-Armstrong, 1996). Only alternating foot structures directly interact with the particles in the transverse tubules, (believed to be the dihydropyridine receptors, DHPRs), suggesting that they are activated

by a mechanism different from that of non-DHPR-associated skeletal RyRs. In cardiac muscle, a lesser level of association between tetrads and foot structures was observed. Thus a direct interaction between cardiac RyRs and DHPR does not seem likely (Franzini-Armstrong, 1996).

The differential role of RyR isoforms in excitation-contraction coupling in skeletal muscle versus heart is still not well understood. An important conclusion of our study is that skeletal and cardiac RyR channel populations differ markedly in their heterogeneity of channel behavior, which may be a consequence of the modulation reflecting depolarization-induced calcium release versus calcium-induced calcium release.

Teflon septa and bilayer chambers used in our experiments were a generous gift from Prof. Hansgeorg Schindler, University of Linz. We thank Prof. H. Schindler and Mr. Alois Sonnleitner for valuable discussion, Dr. Dirk Snyders of Vanderbilt University Medical School for comments on the manuscript, and Ms. Jennifer McConnell for secretarial assistance.

This study was supported by National Institutes of Health grants HL32711 and HL46681, and by a grant from the Muscular Dystrophy Association (to SF).

REFERENCES

Armisén, R., J. Sierralta, P. Vélez, D. Naranjo, and B. Suárez-Isla. 1996. Modal gating in neuronal and skeletal muscle ryanodine-sensitive Ca^{2+} release channels. *Am. J. Physiol.* 271:C144–C153.

Ashley, R. H., and A. J. Williams. 1990. Divalent cation activation and inhibition of single calcium release channels from sheep cardiac sarcoplasmic reticulum. *J. Gen. Physiol.* 95:981–1005.

Barg, S., J. Copello, and S. Fleischer. 1997. Different interactions of cardiac and skeletal muscle ryanodine receptors with FK-506 binding protein isoforms. *Am. J. Physiol.* 272:C1726–C1733.

Bezprozvanny, I., J. Watras, and B. E. Ehrlich. 1991. Bell-shaped calcium-response curves of Ins(1,4,5)P3- and calcium-gated channels from endoplasmic reticulum of cerebellum. *Nature.* 35:751–754.

Blatter, L. A., A. Tsugorka, N. Shirokova, and E. Ríos. 1996. Eager triads in skeletal muscle: heterogeneous distribution of voltage-elicited Ca^{2+} release revealed by confocal microscopy. *Biophys. J.* 70:A235.

Bull, R., and J. J. Marengo. 1993. Sarcoplasmic reticulum release channels from frog skeletal muscle display two types of calcium dependence. *FEBS Lett.* 331:223–227.

Chamberlain, B. K., D. O. Levitsky, and S. Fleischer. 1983. Isolation and characterization of canine cardiac sarcoplasmic reticulum with improved Ca^{2+} transport properties. *J. Biol. Chem.* 258:6602–6609.

Chamberlain, B. K., P. Volpe, and S. Fleischer. 1984. Calcium-induced calcium release from purified cardiac sarcoplasmic reticulum vesicles. General characteristics. *J. Biol. Chem.* 259:7540–7546.

Chu, A., M. Fill, E. Stefani, and M. L. Entman. 1993. Cytoplasmic Ca^{2+} does not inhibit the cardiac muscle sarcoplasmic reticulum ryanodine receptor Ca^{2+} channel, although Ca^{2+}-induced Ca^{2+} inhibition of Ca^{2+} release is observed in native vesicles. *J. Membr. Biol.* 135:49–59.

Colquhoun, D., and A. G. Hawkes. 1995. The principles of the stochastic interpretation of ion-channel mechanisms. *In* Single Channel Recording, 2nd Ed. B. Sakmann and E. Neher, editors. Plenum Press, New York. 397–482.

Copello, J. A., S. Barg, H. Onoue, and S. Fleischer. 1996. Heterogeneity of Ca^{2+} gating of skeletal muscle ryanodine receptor (RyR-1) compared with cardiac RyR-2. *Biophys. J.* 69:164a.

Coronado, R., J. Morrissette, M. Sukhareva, and D. M. Vaughan. 1994. Structure and function of ryanodine receptors. *Am. J. Physiol.* 266: C1485–C1504.

Dulhunty, A. F., P. R. Junankar, K. R. Eager, G. P. Ahern, and D. R. Laver. 1996. Ion channels in the sarcoplasmic reticulum of striated muscle. *Acta Physiol. Scand.* 156:375–385.

Fabiato, A. 1983. Calcium-induced release of calcium from the cardiac sarcoplasmic reticulum. *Am. J. Physiol.* 245:C1–C14.

Fabiato, A. 1988. Computer programs for calculating total from specified free or free from specified total ionic concentrations in aqueous solutions containing multiple metals and ligands. *Methods Enzymol.* 157: 378–417.

Fleischer, S., and M. Inui. 1989. Biochemistry and biophysics of excitation-contraction coupling. *Annu. Rev. Biophys. Biophys. Chem.* 18: 333–364.

Franzini-Armstrong, C. 1996. Ultrastructural studies on feet/ryanodine receptors. *In* Ryanodine Receptors. V. Sorrentino, editor. CRC Press, Boca Raton, FL. 1–16.

Hain, J., S. Nath, M. Mayrleitner, S. Fleischer, and H. Schindler. 1994. Phosphorylation modulates the function of the calcium release channel of sarcoplasmic reticulum from skeletal muscle. *Biophys. J.* 67: 1823–1833.

Hain, J., H. Onoue, M. Mayrleitner, S. Fleischer, and H. Schindler. 1995. Phosphorylation modulates the function of the calcium release channel of sarcoplasmic reticulum from cardiac muscle. *J. Biol. Chem.* 270: 2074–2081.

Harrison, S. M., and D. M. Bers. 1987. The effects of temperature and ionic strength on the apparent Ca-affinity of EGTA and the analogous Ca-chelators BAPTA and dibromo-BAPTA. *Biochim. Biophys. Acta.* 925: 133–143.

Landaw, E. M., and J. J. DiStefano, III. 1984. Multiexponential, multicompartmental, and noncompartmental modeling. II. Data analysis and statistical considerations. *Am. J. Physiol.* 246:R665–R677.

Laver, D. R., L. D. Roden, G. P. Ahern, K. R. Eager, P. R. Junankar, and A. F. Dulhunty. 1995. Cytoplasmic Ca^{2+} inhibits the ryanodine receptor from cardiac muscle. *J. Membr. Biol.* 147:7–22.

Lee, Y. S., K. Ondrias, A. J. Duhl, B. E. Ehrlich, and D. H. Kim. 1991. Comparison of calcium release from sarcoplasmic reticulum of slow and fast twitch muscles. *J. Membr. Biol.* 122:155–163.

Lokuta, A. J., M. B. Meyers, G. I. Fishman, P. R. Sanders, and H. H. Valdivia. 1997. Modulation of cardiac ryanodine receptors by sorcin, a calcium-binding protein of multidrug resistance cells. *Biophys. J.* 72: A333.

Ma, J. 1995. Desensitization of the skeletal muscle ryanodine receptor: evidence for heterogeneity of calcium release channels. *Biophys. J.* 68:893–899.

Marengo, J. J., R. Bull, and C. Hidalgo. 1996. Calcium dependence of ryanodine-sensitive calcium channels from brain cortex endoplasmic reticulum. *FEBS Lett.* 383:59–62.

Mayrleitner, M., A. P. Timerman, G. Wiederrecht, and S. Fleischer. 1994. The calcium release channel of sarcoplasmic reticulum is modulated by FK-506 binding protein: effect of FKBP-12 on single channel activity of the skeletal muscle ryanodine receptor. *Cell Calcium.* 15:99–108.

Meissner, G. 1984. Adenine nucleotide stimulation of Ca^{2+}-induced Ca^{2+} release in sarcoplasmic reticulum. *J. Biol. Chem.* 259:2365–2374.

Meissner, G. 1994. Ryanodine receptor/Ca^{2+} release channels and their regulation by endogenous effectors. *Annu. Rev. Physiol.* 56:485–508.

Nagasaki, K., and M. Kasai. 1983. Fast release of calcium from sarcoplasmic reticulum vesicles monitored by chlortetracycline fluorescence. *J. Biochem.* 94:1101–1109.

O'Brien, J., H. H. Valdivia, and B. A. Block. 1995. Physiological differences between the α and β ryanodine receptors of fish skeletal muscle. *Biophys. J.* 68:471–482.

Ogawa, Y. 1994. Role of ryanodine receptors. *Crit. Rev. Biochem. Mol. Biol.* 29:229–274.

Percival, A. L., A. J. Williams, J. L. Kenyon, M. M. Grinsell, J. A. Airey, and J. L. Sutko. 1994. Chicken skeletal muscle ryanodine receptor isoforms: ion channel properties. *Biophys. J.* 67:1834–1850.

Pessah, I. N., A. L. Waterhouse, and J. E. Cassida. 1985. The calcium-ryanodine receptor complex of skeletal and cardiac muscle. *Biochem. Biophys. Res. Commun.* 128:449–456.

Rousseau, E., and G. Meissner. 1989. Single cardiac sarcoplasmic reticulum Ca^{2+} release channel: activation by caffeine. *Am. J. Physiol.* 256: H328–H333.

Rousseau, E., J. Pinkos, and, D. Saravia. 1992. Functional sensitivity of the native skeletal Ca^{2+}-release channel to divalent cations and the Mg-ATP complex. *Can. J. Physiol. Pharmacol.* 70:394–402.

Saito, A., S. Seiler, A. Chu, and S. Fleischer. 1984. Preparation and morphology of sarcoplasmic reticulum terminal cisternae from rabbit skeletal muscle. *J. Cell Biol.* 99:875–885.

Schindler, H. 1989. Planar lipid-protein membranes: strategies of formation and of detecting dependencies of ion transport functions on membrane conditions. *Methods Enzymol.* 171:225–253.

Sitsapesan, R., and A. J. Williams. 1994. Gating of the native and purified cardiac SR Ca^{2+} release channel with monovalent cation as permeant species. *Biophys. J.* 67:1484–1494.

Smith, J. S., R. Coronado, and G. Meissner. 1986. Single channel measurements of the calcium release channel from skeletal muscle sarcoplasmic reticulum. Activation by Ca^{2+} and ATP and modulation by Mg^{2+}. *J. Gen. Physiol.* 88:573–588.

Sorrentino, V., and P. Volpe. 1993. Ryanodine receptors: how many, where and why? *Trends Pharmacol. Sci.* 14:98–103.

Timerman, A. P., T. Jayaraman, G. Wiederrecht, H. Onoue, A. R. Marks, and S. Fleischer. 1994. The ryanodine receptor from canine heart sarcoplasmic reticulum is associated with a novel FK-506 binding protein. *Biochem. Biophys. Res. Commun.* 198:701–706.

Timerman, A. P., E. Ogunbumni, E. Freund, G. Wiederrecht, A. R. Marks, and S. Fleischer. 1993. The calcium release channel of sarcoplasmic reticulum is modulated by FK-506 binding protein. Dissociation and reconstitution of FKBP-12 to the calcium release channel of skeletal muscle sarcoplasmic reticulum. *J. Biol. Chem.* 268:22992–22999.

Timerman, A. P., H. Onoue, H.-B. Xin, S. Barg, J. Copello, G. Wiederrecht, and S. Fleischer. 1996. Selective binding of FKBP12.6 by the cardiac ryanodine receptor. *J. Biol. Chem.* 271:20385–20391.

Timerman, A. P., G. Wiederrecht, A. Marcy, and S. Fleischer. 1995. Characterization of an exchange reaction between soluble FKBP-12 and the FKBP·ryanodine receptor complex. Modulation by FKBP mutans deficient in peptidyl-prolyl isomerase activity. *J. Biol. Chem.* 270: 2451–2459.

Tripathy, A., L. Xu, G. Mann, and G. Meissner. 1995. Calmodulin activation and inhibition of skeletal muscle Ca^{2+} release channel (ryanodine receptor). *Biophys. J.* 69:106–119.

Tsien, R. Y. 1980. New calcium indicators and buffers with high selectivity against magnesium and protons: design, synthesis, and properties of prototype structures. *Biochemistry.* 19:2396–2404.

Witcher, D. R., R. J. Kovacs, H. Schulman, D. C. Cefali, and L. R. Jones. 1991. Unique phosphorylation site on the cardiac ryanodine receptors regulates calcium channels activity. *J. Biol. Chem.* 266:11144–11152.

Zahradníková, A., J. Bak, and L. G. Mészáros. 1995. Heterogeneity of the cardiac calcium release channel as assessed by its response to ADP-ribose. *Biochem. Biophys. Res. Commun.* 210:457–463.

Zahradníková, A., and I. Zahradník. 1995. Description of modal gating of the cardiac calcium release channel in planar lipid membranes. *Biophys. J.* 69:1780–1788.

Zorzato, F., R. Sacchetto, and A. Margreth. 1994. Identification of two ryanodine receptor transcrips in neonatal, slow-, and fast-twitch rabbit skeletal muscles. *Biochem. Biophys. Res. Commun.* 203:1725–1730.